Surface Tension and Adsorption of Volatile Organic Amphiphiles in Aqueous Solution

by

Andrew Michael Prpich

A thesis

presented to the University of Waterloo

in fulfillment of the

thesis requirement for the degree of

Master of Applied Science

in

Chemical Engineering

Waterloo, Ontario, Canada, 2007

I hereby declare that I am the sole author of this thesis. This is a true copy of this thesis, including any required final revisions, as accepted by my examiners.

I understand that my thesis may be made electronically available to the public.

Andrew Prpich

Abstract

The surface tension of an interface separating two bulk phases is one of the most widely studied properties in surface science research. The importance of surface or interfacial tension is reflected in the diverse number of applications which are influenced by surface tension related effects. This thesis represents a comprehensive experimental and theoretical investigation on molecular adsorption and surface tension from a class of organic compounds in aqueous solutions. The research illustrates the effect of both liquid and vapor phase adsorption on the interfacial properties. Adsorption from both sides of the vapor/liquid interface is considered simultaneously rather than exclusive of one another, which has been the conventional practice.

In the experimental study, the surface tension of a number of different volatile organic compounds is measured using the Axisymmetric Drop Shape Analysis-Profile (ADSA-P) method. The experiments were performed in a controlled environment under conditions where the surface tension can be affected by both vapor and liquid phase adsorption. The vapor phase was exerted by the presence of an environment solution containing the same organic component as in the drop solution. The results show that initially the surface tension is influenced by the organic concentration in both the liquid and the vapor phase. At the final steady-state the liquid phase becomes less important and the primary factor influencing the surface tension is the vapor phase concentration. The ADSA-P technique is verified by reproducing a select number of cases using the Wilhelmy plate method. A possible consequence of the surface tension phenomenon is illustrated through time-dependent contact

angle experiments. The behavior of the interface at steady-state conditions is investigated by measuring the surface tension response to a change in drop volume. It is concluded that the organic compounds considered in the current study may represent a rather general group of molecules whose surface behavior is unique to that of many conventional surfactants.

In the theoretical study an empirical model is proposed to describe the relation between the steady-state surface tension and the concentration of the environment and drop solutions. The results confirm the experimental observation that the final steady-state surface tension is determined primarily by the organic concentration in the vapor phase. In addition, a modified adsorption isotherm is developed to account for simultaneous adsorption from both sides of the vapor/liquid interface at steady-state conditions. The derivation is based upon the classic Langmuir analysis, and the new equation is consistent with the Langmuir isotherm under traditional conditions where adsorption occurs from one side of the interface. The modified isotherm is shown to be consistent with the experimental data and is used to generate the equilibrium parameters for three of the systems studied in this research. The adsorption isotherm is then extended to model the dynamic adsorption process through the creation of a new kinetic transfer equation. As with the adsorption isotherm, the transfer equation is based on Langmuir kinetics and is capable of simulating adsorption from both sides of the interface during surface equilibration. The kinetic transfer equation is validated against experimental data from two systems which exhibit a transfer-controlled adsorption mechanism. The theoretical predictions from the transfer equation fit well with the experimental data for both systems. However, significant variability is observed in the least squares estimates of the kinetic rate constants. The variability is attributed to the limitations of empirical models that

utilize adjustable fitting parameters to optimize the model predictions, and the wide range of surfactant concentrations studied. Specific concentration regions are identified where the variability in the rate constants is minimal and thus, where the model is most appropriate.

Acknowledgements

First, I am extremely grateful to my parents, Mike and Janet Prpich, for their continued love and encouragement. I am deeply indebted to them for all the support they have provided me, financial and emotional, towards my education and growth. There is no doubt that without them I would not be where I am today. I am also thankful for having so many other supportive family members including my sister, Sarah, my grandparents, my cousins, Chris and Tommy, and all my aunts and uncles, especially Tom and Joyce Kirchgasser.

I would like to express my sincere appreciation to my supervisor Dr. Pu Chen for his guidance, support, and direction in this research over the past two years. I would also like to thank Dr. Ali Elkamel for his numerous suggestions and our valuable discussions regarding my research and course work during my time here. I would like to thank the other members of my committee Dr. Rajinder Pal and Dr. G. Wayne Brodland for their careful review of this Master's thesis. I am also grateful to the entire staff of the Chemical Engineering Department at the University of Waterloo, especially Mrs. Pat Anderson and Mrs. Liz Bevan for their help regarding every administrative issue imaginable.

I would like to thank all the current and former members of the Nano-Bio Interfacial Engineering Group, especially Elias, Hank, Nasim, and Maggie, for their advice and assistance during my research. Spending the past two years with them has been quite a learning experience.

Finally, I would like to acknowledge all my friends in Waterloo and elsewhere who have made my life outside of school a nice release from the daily routine. Thanks Matt “Like you didn’t know it was a joke” Elgie, Rolland “Chief Complaining Officer” O’Leary, Chris “When I woke up I was covered in water” Marton, Justin “I can pull off wearing a yellow belt” Fluit, and Heather “We were wearing the same pants” Cruickshank. I especially want to thank Kristina Kowalski for all her love and support. Thanks for being there whenever I needed you.

“You can’t lose what you don’t put in the middle. But you can’t win much either”

Go Pack Go!!

Dedication

To my grandparents

Mike and Julia Prpich, and Tom and Marion Downey

You have been more of an inspiration than you could ever know

Table of Contents

List of Tables

List of Figures

List of Symbols

A	Non-ideality parameter of the Frumkin isotherm (dimensionless)
B	Empirical measure of surfactant interaction at the interface (dimensionless)
β	Empirical surface tension model coefficient
C	Bulk liquid surfactant concentration (mol/m^3)
C_o	Initial bulk liquid surfactant concentration (mol/m^3)
C_{drop}	Concentration of surfactant in the drop solution (mol/m^3)
C_{env}	Concentration of surfactant in the environment solution (mol/m^3)
D	Diffusion coefficient (m^2/s)
Γ	Surface concentration of surfactant (mol/m^2)
Γ_∞	Maximum surface concentration (mol/m^2)
γ	Surface tension of the solution (mN/m)
γ_o	Surface tension of the pure solvent (mN/m)
θ	Contact angle (°)
F	Force acting on the Wilhelmy plate (N)
H	Henry's law constant ($atm \bullet m^3/mol$)
K_H	Henry isotherm equilibrium adsorption constant (m)
k_H^a	Henry isotherm adsorption rate constant (m/s)
k_H^d	Henry isotherm desorption rate constant (s^{-1})
K_L	Langmuir isotherm equilibrium adsorption constant (m^3/mol)
k_L^a	Langmuir isotherm adsorption rate constant ($m^3/mol \bullet s$)
k_L^d	Langmuir isotherm desorption rate constant (s^{-1})

K_F	Frumkin Isotherm equilibrium adsorption constant (m^3/mol)
k_F^a	Frumkin isotherm adsorption rate constant (m/s)
k_F^d	Frumkin isotherm desorption rate constant (s^{-1})
K_1	Modified Langmuir isotherm equilibrium adsorption constant (m^3/mol)
K_2	Modified Langmuir isotherm equilibrium adsorption constant (m^3/mol)
k_a^g	Modified Langmuir isotherm vapor phase adsorption rate constant (m^3/mol•s)
k_a^l	Modified Langmuir isotherm liquid phase adsorption rate constant (m^3/mol•s)
k_d^g	Modified Langmuir isotherm vapor phase desorption rate constant (s^{-1})
k_d^l	Modified Langmuir isotherm liquid phase desorption rate constant (s^{-1})
μ	Chemical potential (J/mol)
P	Partial pressure of surfactant in the vapor phase (atm)
ΔP	Pressure difference across the pendant drop interface (Pa)
π	Pi constant
R	Universal gas constant (J/mol•K)
R_1	Principle radius of curvature (m)
R_2	Principle radius of curvature (m)
r_a^g	Rate of adsorption in the vapor phase (mol/m^2•s)
r_a^l	Rate of adsorption in the liquid phase (mol/m^2•s)
r_d^g	Rate of desorption in the vapor phase (mol/m^2•s)
r_d^l	Rate of desorption in the liquid phase (mol/m^2•s)
S	Total number of adsorption sites at the interface (mol/m^2)
S_o	Number of free adsorption sites at the interface (mol/m^2)
S_1	Number of occupied adsorption sites at the interface (mol/m^2)

T	Absolute temperature (K)
t	Time (sec)
t_p	Thickness of the Wilhelmy plate (m)
τ	Dummy variable in the Ward and Tordai equation (sec)
w_p	Width of the Wilhelmy plate (m)
x	Distance from the subsurface (m)

Chapter 1
Introduction

1.1 Overview of Surface Tension and Adsorption

An interface is a physical boundary that separates two distinct immiscible phases and controls the exchange phenomenon between them. The air/liquid, or vapor/liquid, interface is one which is quite common and thus, is often the subject of much scrutiny. Surface or interfacial tension is widely recognized as one of the most important physicochemical properties of an interface separating two bulk phases. As a result, the study of surface tension and the factors influencing it are crucial to the understanding of many natural phenomena as well as the advancement of numerous technological applications.

In nature, the so-called surface tension effect can be seen as the force that allows insects such as water striders to glide effortlessly on the surface of a still pond, and the beading of a water droplet on the face of a leaf [1, 2]. In environmental science, the lowering of surface tension in cloud droplet solutions, due to dissolved organic compounds from aerosols, has been shown to influence several atmospheric processes such as droplet nucleation, growth, and coalescence. The size and number of the water droplets in a cloud affect its optical properties, which have been directly linked to global climate change [3]. In our lungs natural pulmonary surfactants, made up of a complex mixture of lipids and proteins, play a key role in respiration by stabilizing the lungs for proper breathing. The lung surfactants reduce the surface tension of the aqueous alveolar lining to avoid collapse at the end of expiration and lower the pressure difference required for breathing [4, 5]. In biomechanics, it has recently

been proposed that cell sorting and tissue envelopment in embryonic cells are driven by an equivalent surface or interfacial tension consisting of a combined effect of several force generators. This proposal is contrary to the widely accepted hypothesis that these processes are driven by differential adhesions [6, 7].

More recently surface tension effects have been used to advance various scientific applications in fields such as nanoscale engineering where surface area-to-volume ratios are large and dominant. Capillary action has been utilized in soft lithography to create nano-scale optical components and structures with nontrivial geometry and topology for many micro- and nano-fabrication processes [8, 9]. In nano-fluidics, surface tension driven capillary flows in evaporating thin films have been shown to create line patterns with widths smaller than 100 nm in the presence of foaming surfactants [10]. For inkjet printers, the flow behavior and droplet formation of the ink during the printing process is dominated by surface tension effects. Thus, the surface tension of the working fluids is a critical parameter required to accurately simulate the behavior of an ink droplet in the printhead [11]. Surface tension has also been shown to be a dominant force in nano-scale mechanical systems where it has been utilized to drive the power stroke of a nano-electro-mechanical relaxation oscillator [12].

Surface tension, or surface (excess) free energy, is a tangential force existing at the interface between two phases, caused by the imbalance of cohesive forces on molecules at the surface compared to those in the bulk [13]. In many cases the surface tension of a particular system is highly influenced by the presence of a surface-active-agent, or surfactant. When a fresh interface is formed, the surfactant is drawn toward the interface to achieve a more

thermodynamically stable state as governed by chemical potential and surface activity [13, 14]. The result is a reduction in the surface free energy of the system, and in turn a decrease in surface tension [15]. The surface adsorption is a dynamic process dependent on the type of surfactant and its abundance in the system. Although surface tension has been studied extensively for over a century most research focuses on the effect of the liquid phase surfactant concentration, perhaps because of the much lower density of surfactant in the vapor phase. This justification would be most accurate when a non-volatile system is considered. Although both liquid and vapor phase adsorption are thoroughly examined in almost every Physical Chemistry textbook, they are almost always considered exclusive of one another. However, when a volatile surfactant is dissolved in the liquid phase, which also exerts a finite partial pressure in the vapor phase, can adsorption from both sides of the interface still be considered independent of one another? If not, then to what extent does the vapor phase influence the interfacial properties, as compared to the liquid phase?

To address these questions this research investigates surface tension measurements from a group of slightly volatile, organic amphiphiles in aqueous solutions. The experiments were performed in a controlled environment under conditions where the surface tension can be affected by both vapor and liquid phase surfactant concentrations. Specific attention was paid to the cases where conditions existed for communication (mass transfer) between the liquid and vapor phases. A simple schematic of the system under study is shown in Figure 1.1. A detailed description is given in Chapter 3 of this thesis (Materials and Methods). Previous studies have reported that volatile organic solutions are particularly susceptible to errors during surface tension measurements due to solute evaporation into the vapor phase [16, 17]

and although there have been numerous studies on these particular systems [16-26], the possible influence of the vapor phase on the liquid surface tension has not been considered. Traditionally these organic molecules are referred to as surfactants in the sense that they are surface active and tend to adsorb at an interface. However, this research will illustrate that these systems behave very differently from traditional surfactants in terms of surface tension and adsorption.

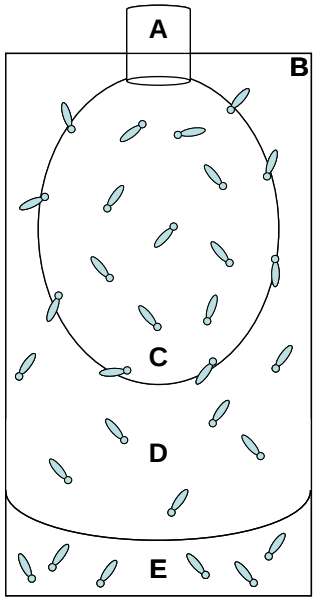

Figure 1.1: A simple schematic of the experimental setup for this research illustrating the key components and the surfactant distribution in the system; (A) capillary tip for drop formation, (B) cuvette for vapor phase control, (C) liquid solution under study (drop solution), (D) vapor phase, (E) external liquid solution (environment solution).

1.2 Research Objectives

The focus of this research is a comprehensive investigation on the influence of vapor phase adsorption on the surface tension of aqueous solutions. In addition to the surface tension measurements, a number of other experimental techniques will be used to confirm the results. A theoretical analysis of the data will also be explored. The major objectives of the research are as follows:

1. Carry out surface tension measurements on a number of volatile, organic amphiphiles in aqueous solution to determine to what extent vapor phase adsorption affects the surface tension in comparison to the liquid phase.
2. Confirm the results from the surface tension experiments using various other experimental techniques for studying surface adsorption, including other surface tension methods and contact angle measurements.
3. Develop a theoretical model that describes the steady-state adsorption behavior of the aqueous surfactant systems.
4. Extend the steady-state analysis to model the dynamic adsorption process of the systems through the creation of a new kinetic transfer equation.
5. Validate both the steady-state and dynamic models using the experimental data.

1.3 Thesis Outline

The material presented in this thesis addresses the objectives outlined in the preceding section. The thesis is organized as follows: In Chapter 2 the theoretical background and literature review of research pertinent to the current body of work, including relevant experimental methods, are presented. In Chapter 3 the chemical materials and experimental methods utilized in this study are described. In Chapter 4 the results from the experimental investigation are presented and discussed. The section includes the surface tension experiments from a number of different systems, a comparison of select results between two different methods, contact angle experiments, and the surface tension response to a change in drop volume. In Chapter 5 the theoretical framework for both the steady-state and dynamic analysis is developed and validated against experimental data. Finally, in Chapter 6 the conclusions from the research are stated and some recommendations are given for future research directions.

Chapter 2

Theoretical Background and Literature Review

In this chapter, the theoretical concepts behind interfacial surfactant adsorption are introduced. The discussion addresses the thermodynamics of adsorption and the Gibbs equation, equilibrium and dynamic adsorption behavior including a detailed overview of several dynamic adsorption models, and various surface tension measurement techniques. Prior research in the area of surface tension and adsorption is also presented.

2.1 Adsorption at an Interface

For adsorption to occur spontaneously at an interface two important conditions must be satisfied. First, two immiscible bulk phases must be in direct contact with each other for transfer to occur. Second, one or both of the phases must contain more than one component. The process of transfer of the component (adsorbate) from the bulk to the interface will continue until a state of adsorption equilibrium is reached. In a liquid system the adsorption depends on the composition of the solution and both solute and solvent components in the bulk medium compete with each other for excess accumulation at the interfacial region [15]. The thermodynamics of surface excess accumulation for different types of adsorption phenomenon at fluid interfaces are described by the universal concept of "the Gibbs surface excess".

2.1.1 Thermodynamics of Adsorption: The Gibbs Equation

In the his classic publication [27], J.W. Gibbs derived the general equations governing adsorption at interfaces including the legendary Gibbs adsorption equation. He considered a

liquid column containing two bulk phases α and β separated from each other by a surface region (Figure 2.1) [15]. Because the actual surface region is inhomogeneous and thus hard to define, Gibbs simplified the system by considering an idealized liquid column where the two phases α and β are separated not by an actual interfacial phase but by an arbitrary dividing plane (Figure 2.2). The plane is chosen such that the compositions of the two phases remain unchanged right up to the dividing surface.

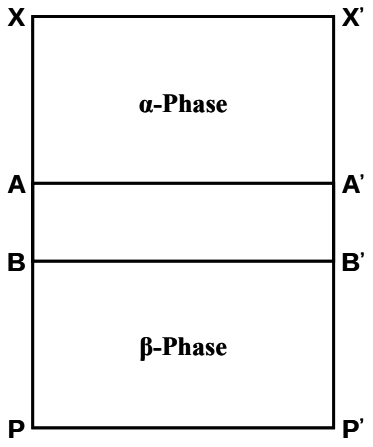

Figure 2.1: The liquid column in the real system [15]**.**

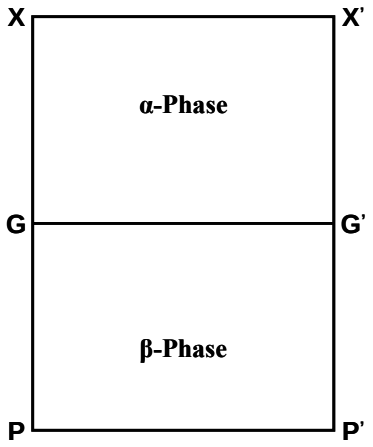

Figure 2.2: The liquid column in the idealized system [15]**.**

This simplification allowed Gibbs to define the surface excess quantities of the species at the interface. Using a thermodynamic treatment he was able to derive the following equation for a binary system at constant temperature [13]:

$$d\gamma = -\Gamma_1 d\mu_1 - \Gamma_2 d\mu_2 \qquad (2.1)$$

where γ is the surface tension, Γ_1 and Γ_2 are the surface excess concentrations of the solvent and the solute, respectively, and μ_1 and μ_2 are the chemical potentials of the solvent and the solute, respectively. Since Γ_1 and Γ_2 are defined relative to the arbitrarily chosen dividing surface, it is possible in principle to position the surface such that $\Gamma_1 = 0$, so that:

$$\Gamma_2 = -\left(\frac{d\gamma}{d\mu_2}\right)_T \tag{2.2}$$

Utilizing the ideal dilute solution assumption, one can set the activity coefficients to unity and relate the mole fractions to concentration. Equation (2.2) becomes:

$$\Gamma_2 = -\frac{1}{RT}\left(\frac{d\gamma}{d\ln C_2}\right) \tag{2.3}$$

where C_2 is the concentration of the solute in the liquid phase, R is the universal gas constant, and T is the absolute temperature. Equation (2.3) is the simplest form of the Gibbs adsorption equation which relates the change in surface tension to the surface excess accumulation or adsorption. If the derivative in Equation (2.3) is negative then Γ_2 is positive and there is a surface excess of solute. If the derivative is positive then there is a surface deficiency of solute. If a solute is positively adsorbed it will result in a decrease in surface tension.

2.1.2 Equilibrium Adsorption Isotherm

The purpose of an adsorption isotherm is to relate the surfactant concentration in the bulk and the amount adsorbed at the interface [28]. A number of the most commonly used adsorption isotherms will be discussed here. For a single component system, the simplest isotherm is the Henry isotherm (or Henry's law isotherm) which is a linear relation between the surface excess and the bulk surfactant concentration:

$$\Gamma = K_H C \tag{2.4}$$

where Γ is the surface excess concentration of surfactant, K_H is the Henry equilibrium adsorption constant, and C is the concentration of surfactant in the bulk liquid phase. The equilibrium adsorption constant is an empirical measure of the surface activity of the surfactant and thus, a critical parameter in any isotherm [28, 29]. The Henry isotherm is valid

for low surface concentrations where interactions between species at the interface are insignificant. The obvious drawback of the isotherm is that there is no limitation on the maximum value of Γ.

The most commonly used non-linear isotherm is the Langmuir isotherm:

$$\Gamma = \Gamma_{\infty} \frac{K_L C}{1 + K_L C} \tag{2.5}$$

where Γ_{∞} is the maximum surface concentration and K_L is the Langmuir equilibrium adsorption constant. The parameter Γ_{∞} is the theoretical limit of the surface concentration which typically is not attainable due to constraints on C, such as the solubility or the critical micelle concentration (cmc). The Langmuir isotherm is based on a lattice-type model where every adsorption site on the lattice is equivalent. Also, the probability for adsorption at an empty site is independent of the occupancy of the neighboring sites and there are no interactions or intermolecular forces acting between the species in the lattice [28]. This last point is also the main limitation of the Langmuir isotherm. Many species exhibit intermolecular interactions at the interface, which can include relatively weak van der Waals forces, or stronger interactions due to electrostatic effects or hydrogen bonding. Thus, the adsorption and desorption rates can be affected (positively or negatively) as the surface coverage increases.

The Frumkin isotherm builds on the Langmuir equation by attempting to account for solute-solvent interactions at a non-ideal surface [29]. It is most appropriate for non-ionic surfactants and is usually presented in the following form:

$$C = \frac{1}{K_F}\frac{\Gamma}{\Gamma_\infty - \Gamma}\exp\left[-A\left(\frac{\Gamma}{\Gamma_\infty}\right)\right] \tag{2.6}$$

where K_F is the Frumkin equilibrium adsorption constant, and A is a measure of the non-ideality of the surface layer. The parameter A essentially serves as an estimate of the influence of molecular attractions or repulsions between surfactant molecules at the interface on the surface concentration. If A = 0, the surface layer is considered ideal, and the equation reduces to the Langmuir isotherm.

Although most of these isotherms are best suited for non-ionic surfactants, Borwankar and Wasan extended the Frumkin isotherm to account for effects of the electric double layer for ionic surfactants [30]. The subsurface concentration is corrected for electric double layer effects using Boltzmann factors and the formulation is applicable to both cationic and anionic surfactants. Recently, Lin et al. have used an activation energy barrier approach to account for enhanced intermolecular interaction at increasing surface coverage [23-25]. The activation energies are assumed to follow a power law dependence on the surface coverage (Γ). The presence of cohesive intermolecular forces, which increase with surface coverage, lower the desorption rate relative to the rate of adsorption.

2.1.3 Surface Equation of State

Once the proper isotherm is chosen, the Gibbs adsorption equation can be used to derive the corresponding surface equation of state for a given system. The purpose of the equation of state is to eliminate the surface concentration (Γ) from the adsorption isotherm and relate the surface tension directly to the surfactant concentration in the bulk (C). The following

equations apply to premicellar dilute solutions only (C < cmc) so that the chemical potential can be aptly represented by concentration in the Gibbs adsorption equation.

A simple linear surface equation of state, corresponding to the Henry isotherm, is given below:

$$\gamma = \gamma_o - RTK_H C \tag{2.7}$$

where γ and γ_o are the surface tensions of the solution and pure solvent, respectively.

The analogous forms of the surface equation of state for the Langmuir isotherm are the Frumkin equation (not to be confused with the Frumkin isotherm) and the Szyszkowski equation respectively, given below [28, 29]:

$$\gamma = \gamma_o + RT\Gamma_\infty \ln\left(1 - \frac{\Gamma}{\Gamma_\infty}\right) \tag{2.8}$$

$$\gamma = \gamma_o - RT\Gamma_\infty \ln\left(1 + K_L C\right) \tag{2.9}$$

The corresponding surface equation of state for the Frumkin isotherm is [28, 29]:

$$\gamma = \gamma_o + RT\Gamma_\infty \ln\left(1 - \frac{\Gamma}{\Gamma_\infty}\right) + \tfrac{1}{2} RTA\Gamma_\infty \left(\frac{\Gamma}{\Gamma_\infty}\right)^2 \tag{2.10}$$

Examining Equation (2.6) and (2.10) it is clear that a relation between γ and C exists, involving the three parameters Γ_∞, K_F, and A. However, due to the nonlinearity of these equations, no analytical expression for γ(C) can be derived, and the solution can only be determined numerically.

2.1.4 Determination of Equilibrium Adsorption Parameters

By applying a suitable surface equation of state, one can determine the equilibrium adsorption parameters for a given system through nonlinear regression with experimental data of surface tension vs. concentration. Typically, a curve fitting method is used where the parameters are generated by minimizing the sum of squared error between the experimental data and the theoretical predictions. Since the adsorption isotherm is derived based on steady-state or equilibrium conditions, the parameters must be generated using data collected at steady-state conditions. The equilibrium adsorption parameters give important insight into the physical properties of a given surfactant, as well as the validity of the adsorption isotherm and surface equation of state.

As stated previously, the equilibrium adsorption constant (e.g. K_L for the Langmuir isotherm) is used as a measure of the surface activity of a surfactant. Therefore, it is a key parameter for differentiating surfactant efficiency (i.e. a surfactants ability to lower the surface tension) since greater surface activity means higher efficiency. For hydrocarbon based surfactants the surface activity typically increases with chain length, indicating that longer surfactants are more surface active [29]. In general, Γ_∞ does not vary dramatically for different surfactants, especially those of similar structure. However, the maximum surface coverage will usually increase slightly with hydrocarbon chain length. The non-ideality parameter in the Frumkin isotherm (A) is highly dependent on the nature of the surfactant. It can be interpreted in terms of repulsive or attractive interactions between the functional group(s) on the surfactant, and water molecules or adjacent surfactant molecules [29].

2.2 Mechanisms of Surfactant Adsorption

When a fresh surface of a surfactant solution is formed, the equilibrium surface tension is not achieved instantly. A finite time is required to reach equilibrium between the surface concentration and the bulk surfactant concentration [29]. The non-equilibrium surface tension is called the Dynamic Surface Tension (DST), and is dependent on the type of surfactant and its composition in the system. The mechanism for the adsorption of a soluble surfactant from a liquid solution can consist of three physical steps, which are illustrated in Figure 2.3. The first step involves exchange of the component between the bulk solution and the subsurface layer (located immediately below the surface layer, a few molecular diameters thick). The second step entails transfer of the component between the subsurface and the surface layer. In the final step, the component rearranges itself at the surface to an equilibrium state. For small molecules, rearrangement is generally a fast process and has little effect on the overall adsorption behavior [31]. The first step is a bulk mass transfer process (usually diffusion) and the second step is an adsorption process [29].

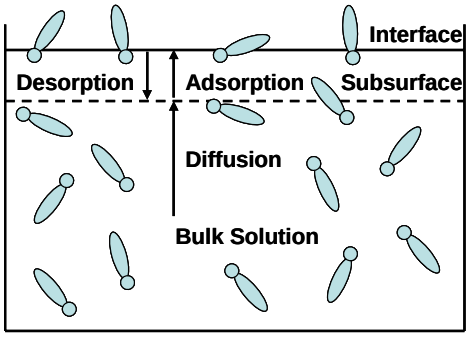

Figure 2.3: A schematic diagram of the dynamic adsorption mechanism.

The adsorption kinetics are typically characterized based on the rate-limiting step of the outlined process. For example, the adsorption is said to be diffusion-controlled if the first

step is much slower than the transfer step. If transfer between the subsurface and the interface is rate-limiting then the process is said to be transfer-controlled. If the characteristic times for the first two steps are comparable, then the process is said to be mixed diffusion/transfer-controlled.

2.2.1 Diffusion-Controlled Adsorption

For diffusion-controlled adsorption it is assumed that there is no activation energy barrier to transfer between the subsurface and the interface [29]. Therefore, every molecule arriving at the subsurface immediately finds an empty site and adsorbs directly to the interface. This assumption is most valid for a short time after a fresh interface is formed when the surface concentration is low. The situation is known as the local equilibrium model in which the surface concentration is always in equilibrium with the subsurface concentration. For the simplest unsteady, one-dimensional problem, the diffusion can be represented by Fick's 2nd law equation:

$$\frac{\partial C}{\partial t} = D\frac{\partial^2 C}{\partial x^2} \tag{2.11}$$

The system has the following initial and boundary conditions:

$$C(x,0) = C_o \tag{2.12}$$

$$\Gamma(0) = 0 \tag{2.13}$$

$$C(\infty,t) = C_o \tag{2.14}$$

where C is the surfactant concentration, C_o is the initial bulk concentration, Γ is the surface concentration, D is the diffusion coefficient, t is the time, and x is the distance from the subsurface. Using the technique of Laplace transform Equations (2.11) – (2.14) can be solved to obtain:

$$\Gamma(t) = 2C_o\sqrt{\frac{Dt}{\pi}} - \sqrt{\frac{D}{\pi}}\int_0^t \frac{C(0,\tau)}{\sqrt{t-\tau}}d\tau \qquad (2.15)$$

where $\pi = 3.1415$ and τ is a dummy variable. This equation, derived by Ward and Tordai in 1946 [32], was the first quantitative model for surfactant adsorption by a diffusion-only mechanism. The second term in Equation (2.15) accounts for the slowing of diffusion as the subsurface concentration increases (also known as back-diffusion). Due to the integral term, no analytical solution is available for the Ward and Tordai equation. However, limiting laws have been used to approximate the solution when $\gamma(t)$ is close to the solvent (γ_o), or when it is close to the equilibrium value (γ_{eq}). These are the asymptotic equations given by Miller et al. [33], and their solutions are outlined below.

The first limiting law is called the short time approximation ($t \rightarrow 0$). Initially, when the subsurface concentration is low, the back diffusion integral can be neglected. This simplification gives:

$$\Gamma(t) = 2C_o\sqrt{\frac{Dt}{\pi}} \qquad (2.16)$$

Since the solution can be treated as dilute for the short time approximation, the linear Henry isotherm can be used to relate Γ and γ:

$$\gamma_{t\rightarrow 0} = \gamma_o - 2RTC_o\sqrt{\frac{Dt}{\pi}} \qquad (2.17)$$

The second limiting law is called the long time approximation. As $t \rightarrow \infty$ the subsurface concentration will tend towards the bulk concentration, and can be factored outside the back

diffusion integral. As a result, the integral term approaches unity as $t \rightarrow \infty$ and the equation can be simplified as follows:

$$C_o - C = \Gamma\sqrt{\frac{\pi}{4Dt}} \tag{2.18}$$

By applying the Gibbs adsorption equation, the long time approximation can be stated as:

$$\gamma_{t\rightarrow\infty} - \gamma_{eq} = \frac{RT\Gamma^2}{C}\sqrt{\frac{\pi}{4Dt}} \tag{2.19}$$

The above equations, as well as various numerical solutions of the Ward and Tordai equation, have been used to describe systems that exhibit diffusion-controlled adsorption. The next section will outline the solutions for mixed control kinetics.

2.2.2 Mixed Diffusion/Transfer-Controlled Adsorption

In the mixed diffusion/transfer-controlled adsorption mechanism, the surfactant is exchanged between the bulk liquid and the subsurface, obeying the same diffusion equations outlined in the previous section. However, once at the subsurface the surfactant is not instantaneously adsorbed to the interface. This means that the condition of local equilibrium between the subsurface and the interface is no longer valid. Typically, the energy barrier in the adsorption/desorption step is accounted for through the use of a kinetic expression [29]:

$$\frac{d\Gamma}{dt} = r_a - r_d \tag{2.20}$$

where r_a and r_d are the rates of adsorption and desorption, respectively. The kinetic transfer equation describes the change in surface concentration with time. It must also be able to describe the adsorption behavior at equilibrium (i.e. when $d\Gamma/dt = 0$). Therefore, in an appropriate mixed control model the kinetic transfer equation must be consistent with the

equilibrium adsorption isotherm at steady-state conditions. Some of the most commonly used kinetic equations are outlined below.

A simple linear kinetic expression that is consistent with the Henry isotherm at equilibrium is the following:

$$\frac{d\Gamma}{dt} = k_H^a C(0,t) - k_H^d \Gamma \tag{2.21}$$

where k_H^a and k_H^d are the adsorption and desorption rate constants for the Henry kinetic equation, respectively. As with the Henry isotherm, this kinetic equation is suitable only for dilute solutions.

The simplest expression that follows Langmuir kinetics and leads to the Langmuir isotherm at equilibrium is as follows [28, 34]:

$$\frac{d\Gamma}{dt} = k_L^a C(0,t)\left(\Gamma_\infty - \Gamma\right) - k_L^d \Gamma \tag{2.22}$$

In the Langmuir equation the rate of adsorption is proportional to the subsurface concentration and the number of vacant adsorption sites at the interface, while the rate of desorption is proportional to the surface concentration. Evaluation of the expression at equilibrium reveals the relation between the adsorption and desorption rate constants (k_L^a and k_L^d) and equilibrium adsorption constant (K_L):

$$K_L = k_L^a \Big/ k_L^d \tag{2.23}$$

A second kinetic expression, which reduces to the Langmuir isotherm at equilibrium, is the Langmuir-Hinshelwood (L-H) equation [29]:

$$\frac{d\Gamma}{dt} = k_L^a C(0,t)\left(1-\frac{\Gamma}{\Gamma_\infty}\right) - k_L^d \Gamma \tag{2.24}$$

This equation has one slight modification from the Langmuir kinetic equation. In the L-H equation the rate of adsorption is proportional to the subsurface concentration and the fraction of vacant adsorption sites at the interface rather than the number of available sites. The relation between k_L^a, k_L^d and K_L at equilibrium is:

$$K_L = k_L^a \Big/ k_L^d \Gamma_\infty \tag{2.25}$$

A further modification of the Langmuir-Hinshelwood equation was proposed by Chang and Franses to account for the effect of surface coverage on the rate of adsorption from the subsurface [19]:

$$\frac{d\Gamma}{dt} = k_L^a C(0,t)\left(1-\frac{\Gamma}{\Gamma_\infty}\right)\exp\left(-B\frac{\Gamma}{\Gamma_\infty}\right) - k_L^d \Gamma \exp\left(-B\frac{\Gamma}{\Gamma_\infty}\right) \tag{2.26}$$

In the modified L-H equation the parameter B is an empirical measure of surfactant interaction at the interface. If B is negative there is a cooperative effect for adsorption and if B is positive there is an anti-cooperative effect for adsorption. The exponential term is compatible with an activation energy barrier concept. The assumption with the modified L-H equation is that the surface coverage has the same effect on the rate of adsorption and desorption. Otherwise, the Langmuir isotherm would not be satisfied at equilibrium.

The kinetic equation consistent with the Frumkin isotherm is [29]:

$$\frac{d\Gamma}{dt} = k_F^a C(0,t)\left(1-\frac{\Gamma}{\Gamma_\infty}\right) - k_F^d \Gamma \exp\left(-A\frac{\Gamma}{\Gamma_\infty}\right) \tag{2.27}$$

The Frumkin equation implies that the interaction parameter A only affects the desorption rate. The adsorption and desorption rate constants (k_F^a and k_F^d) are related to K_F by an expression similar to the modified L-H equation:

$$K_F = k_F^a / k_F^d \Gamma_\infty \tag{2.28}$$

2.2.3 Summary

For diffusion-controlled adsorption models the surface concentration Γ(t) is always in equilibrium with the subsurface concentration C(0,t), which changes as diffusion occurs. Therefore, the equilibrium adsorption isotherm (Section 2.1.2) is used to describe the relationship between C(0,t) and Γ(t). For mixed control kinetics the rate of diffusion is comparable to the rate of adsorption/desorption. In this case, the diffusion equation and the transfer equation must be solved simultaneously. The diffusion equation gives the subsurface concentration of surfactant as a function of time, which is then used to solve for the surface concentration Γ(t) using the appropriate kinetic transfer equation. The third possibility is that the rate of diffusion is fast and the adsorption/desorption step is rate-limiting. This situation is called transfer-controlled adsorption and the entire process can be modeled using an appropriate kinetic transfer equation. Since the rate of diffusion is fast, the subsurface concentration at any time t is assumed to be equal to the initial bulk concentration C_o. The transfer equation is then used to solve for the surface concentration Γ(t). A fourth possibility occurs when the time-scale for rearrangement at the interface becomes significant and can no longer be ignored. Typically this situation applies to the adsorption of complex molecules such large proteins or other biological compounds, and is accounted for with a mixed control model that incorporates the rearrangement step [35-37]. Since in this study the focus is on

compounds with relatively small, simple structures, the rearrangement step should not have a significant influence on the adsorption process.

Once the surface concentration is known, a relationship between $\Gamma(t)$ and $\gamma(t)$ is needed since most of the experimental data are for dynamic surface tension rather than surface concentration. A generally accepted assumption in the literature is that the relationship is the same as at equilibrium [29]. The surface equation of state $\gamma(\Gamma)$, obtained from the Gibbs adsorption equation, is used to relate the surface concentration to surface tension as a function of time.

The following paragraphs outline the mechanisms reported in the literature for describing the adsorption of surfactants at a liquid interface. It is limited to a discussion of those studies involving species of organic, amphiphilic nature since these components are the primary focus of this thesis.

Chang and Franses [19, 20] presented dynamic surface tension data for aqueous 1-propanol, 1-heptanol, and 1-octanol. For short adsorption times they found that the adsorption of 1-propanol could be described by a mixed diffusion/transfer-controlled model using the Langmuir-Hinshelwood kinetic equation. For 1-heptanol and 1-octanol a cooperative effect for adsorption was observed with increasing surface coverage. Therefore, the modified Langmuir-Hinshelwood equation was used in a mixed control model to describe the adsorption process. Conversely, Lin et al. [25] report that the adsorption of 1-octanol is diffusion-controlled. They model the dynamic surface tension data using the diffusion

equation coupled with a generalized Frumkin equilibrium isotherm, based on an activation energy barrier approach.

Lin et at. [23, 24] apply a similar theoretical framework to dynamic surface tension data from aqueous 1-decanol. They assume that the adsorption is diffusion-controlled and model the data using the diffusion equation coupled with a generalized Frumkin isotherm, which accounts for intermolecular attraction between surfactant molecules at the interface. Their model fits the data reasonably well and suitable values are obtained for the diffusion coefficient. However, they do not investigate whether a mixed diffusion/transfer-controlled model would improve the fit of their model at short adsorption times when the surface concentration is low.

Joos et al. [18, 38] presented dynamic surface tension data from a number of normal alcohols from propanol to decanol. They found that for the lower alcohols (propanol to pentanol) the adsorption followed a transfer-controlled mechanism and they observed good agreement with the Langmuir-Hinshelwood kinetic equation. For the middle alcohols (hexanol and heptanol) the adsorption shifted to a mixed diffusion/transfer-controlled mechanism and the diffusion equation was incorporated into the model to describe the data. For the higher alcohols (octanol to decanol) the rate-limiting step was found to be diffusion to the subsurface and the adsorption was described by a diffusion-controlled mechanism. In contrast, Fainerman and Miller [21] report that the adsorption kinetics of short-chain alcohols (propanol, butanol, pentanol, and hexanol) at short adsorption times can be described by a diffusion-controlled mechanism and no adsorption barrier needs to be assumed. They apply an approximate

solution of the diffusion equation, which considers the effects of a non-equilibrium surface layer on the dynamic surface tension.

2.3 Experimental Methods for Determining Surface Tension

Over the past century a number of different methods have been developed for measuring the surface tension of a liquid solution [13]. They can be classified into four categories according to the principle that the measurement is based on: (i) force methods – the Du Noüy ring and the Wilhelmy plate; (ii) shape methods – the sessile drop, the pendant drop, or the pendant bubble method; (iii) pressure methods – the maximum bubble pressure method; and (iv) other methods – oscillating jet and drop volume method. Some of these techniques are discussed briefly in the following section. The methods used in this research will be discussed in detail in Chapter 3.

2.3.1 Du Noüy Ring Method

In this method, the capillary force on a platinum ring at the gas/liquid surface is measured. The maximum force required to detach the ring from the liquid surface is proportional to the surface tension, the contact angle, and the wetted perimeter of the ring. A correction factor, based on the ring dimensions, is typically needed in order to obtain accurate results. Since a fresh surface is formed as the ring is pulled upward, the measured tension corresponds to short adsorption times. Therefore, this method is not recommended for measuring dynamic surface tension and should only be applied to rapidly equilibrating systems. Furthermore, surfactant adsorption on the wetted portion of the ring can significantly affect the measured surface tension of some systems.

2.3.2 Wilhelmy Plate Method

Similar to the Du Noüy ring, the Wilhelmy plate method is based on a force measurement. In this case, the force acting on a rectangular plate partially immersed in a liquid solution can be related to the surface tension according to the following equation:

$$F = \gamma P \cos \vartheta \tag{2.29}$$

where F is the measured force, P is the perimeter of the plate, and θ is the contact angle of the liquid on the plate. The plate is usually made of platinum which has been roughened so that the contact angle between the liquid and the plate is zero (i.e. complete wetting). Another popular choice is to use a rectangular piece of filter paper. When used as a detachment method, the issues with this technique are the same as the Du Noüy ring. However, if the plate is kept steady as the tension is measured, and if the contact angle is known or constant, then this method can yield reliable results for dynamic or equilibrium surface tension measurements on most systems.

2.3.3 Maximum Bubble Pressure Method

The maximum bubble pressure method has been used extensively to measure the dynamic surface tension of surfactant solutions. A comprehensive review of this method including apparatus design is given by Mysels [39]. In this method, the maximum pressure necessary to release a bubble from the tip of a capillary, which is calibrated and immersed at a known depth in a liquid solution, is measured. To measure the dynamic surface tension, the pressure in the capillary is maintained constant and the interval between successive bubbles is measured. By varying the pressure, the rate of change of the solution surface tension with time can be determined indirectly.

2.3.4 Oscillating Jet Method

In the oscillating jet method, the solution is ejected through a noncircular orifice under constant pressure. The initial elliptical cross-section of the jet emerging from the orifice is unstable and it oscillates around its equilibrium cross-section. The frequency is determined by the surface tension and the flow parameters; the larger the wavelength of the oscillation, the lower the surface tension. For dynamic surface tension, the wavelength of successive waves increases as the surface tension decreases. The oscillating jet method is best suited for measuring the surface tension of rapidly equilibrating systems (1 – 100 ms). A detailed review of this method has been given by Defay and Petre [40].

2.3.5 Drop Weight Method

This simple and fairly accurate method is one of the oldest for measuring the surface or interfacial tension of a liquid solution. The procedure is to form drops of a liquid at the tip of a capillary, counting the number that fall into a container until enough have been collected to accurately determine the weight per drop. The relationship between the weight of the drop and the surface tension is given by Tate's law [13]:

$$W = mg = 2\pi r\gamma f \tag{2.30}$$

where m is the mass of the drop, g is the gravity constant, r is the capillary tip radius, and f is a correction factor which accounts for the fact that when a drop reaches the point of instability only a portion of the drop actually falls. As much as 40% of the liquid may remain attached to the tip. Values of the correction factor are given by Harkins and Brown [41]. The drop weight method can be used to study dynamic adsorption processes occurring over intervals of seconds to minutes.

2.3.6 Drop and Bubble Shape Methods

In these methods, the surface tension of a solution is determined based on the shape of a liquid drop (or bubble formed inside the solution). The drop can be hanging from a capillary tip (pendant drop) or formed on a flat surface (sessile drop). The shape of the drop is determined by a combination of surface tension and gravity effects. Gravity tends to elongate the drop in the pendant case or spread the drop in the sessile case, while surface tension tends to make the drop more spherical. When the surface tension is reduced due to surfactant adsorption, the gravity effects become more pronounced causing the shape of the drop to evolve over time. The shape will continue to change as surfactant accumulates at the interface and the surface tension is reduced. The dynamic surface tension can be studied with the use of an automated image analysis system. Due to the dead time during the formation of the drop, this method is best suited for systems changing little over the first few seconds. The drop shape methods have become quite popular due to the fact that they are extremely accurate and only small amounts of liquid are required for the measurement.

Chapter 3

Materials and Experimental Methods

3.1 Materials and Sample Preparation

All chemicals for this research (1-butanol, 1-hexanol, 1-octanol, 1-decanol, 1-octylamine, 1-octanoic acid, $C_{12}E_8$, and Igepal-CO-720) were purchased from Sigma-Aldrich Canada (Oakville, Ontario). Estimated water solubility [42-44] and vapor pressure data [45-48] for the organic amphiphiles is given in Table 3.1. The purity was greater than 99% in all cases and no further purification was performed before use. The water used for solution preparation was purified by an Ultra-Pure Water System from Millipore Ltd. (Mississauga, Ontario). The resistivity of the water after purification was measured to be at least 18.2 MΩ and the surface tension was 72.5 ± 0.5 mN/m. For the surfactant solutions, the sample with the highest concentration was prepared first and dilutions were made to the lower concentrations. The highest concentration was chosen to be close to the solubility of the surfactant and the range typically spanned one or two orders of magnitude lower. Samples were tested shortly after preparation and stored for no longer than two weeks. New samples were prepared as necessary.

Table 3.1: Water solubility and vapor pressure data of chemicals under study.

Chemical	Water Solubility (mol/m^3)	Vapor Pressure (mm Hg)
1-butanol	1058.44	5.02 (20°C)
1-hexanol	57.83	0.863 (25°C)
1-octanol	4.15	0.083 (25°C)
1-decanol	0.234	8.25 (100°C)
1-octanoic acid	4.72	0.008 (25°C)
1-octylamine	34.67	15 (70°C)

3.2 Surface Tension Measurements

3.2.1 Axisymmetric Drop Shape Analysis-Profile

The majority of the surface tension measurements were performed using the Axisymmetric Drop Shape Analysis-Profile (ADSA-P) method. In this technique the surface tension is determined based on the shape of an axisymmetric pendant drop. Essentially, the shape of the drop is dictated by a combination of surface tension and gravity effects. Surface tension forces tend to make the drop spherical, whereas gravity tends to elongate the drop [14]. The theoretical shape of the pendant drop is given by the Laplace equation of capillarity which relates the pressure difference across the curved liquid interface to the surface tension and the curvature of the interface [49]:

$$\Delta P = \gamma\left(\frac{1}{R_1} + \frac{1}{R_2}\right) \tag{3.1}$$

where γ is the surface tension, R_1 and R_2 are the two principle radii of curvature, and ΔP is the pressure difference across the interface. The ADSA-P method compares the experimental drop profile to the theoretical solution of Equation (3.1). An objective function arises which expresses the deviation of the experimental profile from the theoretical one as a sum of squares of the normal distances between the experimental points and the calculated curve [14]. The objective function is minimized numerically using a combination of the Newton-Raphson and Levenberg-Marquardt methods and the surface tension is generated as a fitting parameter [50]. The program requires a manual input of the location of the base of the drop (i.e. the cut-off coordinates of the capillary tube), the value of the density difference across the interface, and the magnitude of the local gravitational constant. The solution of the

ADSA-P program yields the surface tension, the volume, the surface area, and the radius of curvature of the pendant drop.

A schematic diagram of the experimental setup for the surface tension experiments is shown in Figure 3.1A. An IsoStation vibration isolated workstation was used to prevent vibration of the key components during operation. An optical light source filtered by a diffuser was used to illuminate the pendant drop. The drop was formed by means of a motorized syringe pump attached to a Hamilton gas-tight syringe. The drop was formed inside a clear quartz cuvette, placed inside the environmental chamber, to allow for control of the vapor phase conditions. The environmental chamber was used to control the temperature of the system and minimize vapor leakage during operation. The drop images were captured by a high speed camera and microscope system that displayed the profile on a monochromatic monitor and exported the image files to a computer system. The digitized images were analyzed using the ADSA-P program once the experiment was completed to generate the surface tension values. A sample drop image is shown in Figure 3.1B.

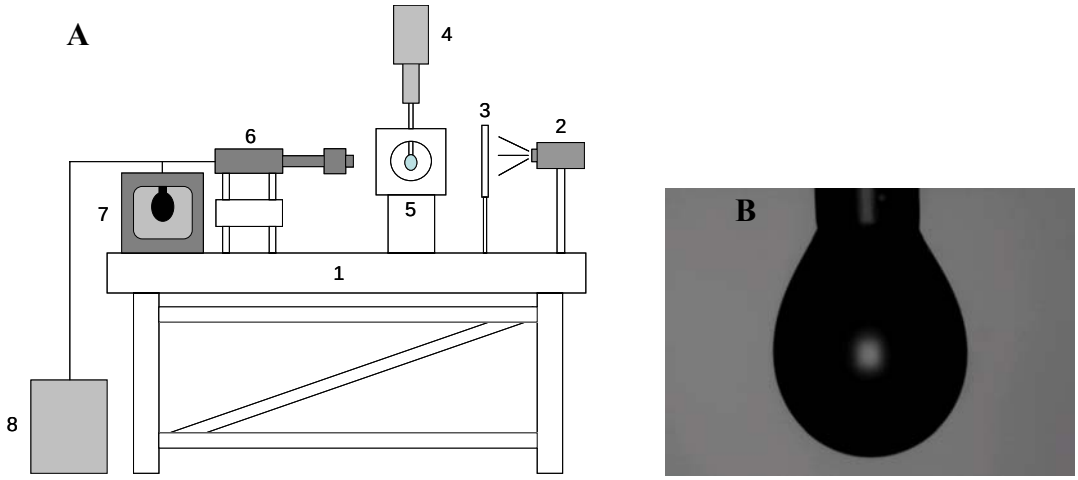

Figure 3.1: (A) Schematic of experimental setup; (1) IsoStation vibration isolated workstation, (2) optical light source, (3) light diffuser, (4) motorized syringe pump and gas-tight syringe, (5) environmental chamber, (6) high speed camera, (7) monochromatic monitor, and (8) computer system. (B) Sample pendant drop image used by the ADSA-P program for surface tension determination.

For each experiment, the pendant drop of the sample under test (referred to as the drop solution) was formed inside the quartz cuvette above 1 ml of aqueous solution (referred to as the environment solution) containing the same component as the drop. The environment solution was added to facilitate adsorption from the vapor side of the interface by creating a surfactant vapor phase surrounding the drop solution. If the two liquid solutions had different surfactant concentrations, a driving force was established for molecular transfer across the vapor/liquid interface causing the surface tension of the drop solution to evolve as a result of the exchange. Before each set of experiments, the gas-tight syringe was cleaned by ultrasonic and repeated rinsing with purified water. After cleaning, approximately 0.3-0.4 ml of aqueous solution was drawn into the syringe. The environment solution was added to the cuvette using a 1 ml micropipette. The syringe was then fed into the cuvette and the environmental chamber was sealed. The system was allowed to equilibrate for 15 minutes, after which the drop was formed using the motorized syringe. The temperature of the

chamber was controlled by a water cooling bath. For the 1-butanol experiments the temperature was set at 25 °C and for all other experiments the temperature was set at 20 °C. Image capture began immediately after the drop was formed and continued until the surface tension of the drop was no longer changing (~2-5 hours). After each use the cuvette was cleaned by rinsing with THF and purified water, and dried with filtered air.

3.2.2 Wilhelmy Plate Method

To provide confirmation of the surface tension results obtained by the ADSA-P method, select cases were repeated with the Wilhelmy plate method. In this technique the surface tension is determined based on the force acting on a rectangular plate that is partially immersed in the solution under test [13]. The components making up the overall force acting on the plate (F) can be related to the surface tension according to the following equation [51]:

$$F = p\gamma \cos\theta - \rho g V \tag{3.2}$$

where p is the wetted perimeter of the plate, γ is the surface tension of the solution, θ is the contact angle of the liquid on the Wilhelmy plate, ρ is the liquid density, g is the local gravitational constant, and V is the volume of the plate immersed in the solution. The first term on the right-hand side of Equation (3.2) is the force due to the surface tension, while the second term is the buoyancy force. If the plate is positioned so that the lower edge is level with the surface of the liquid, the buoyancy force is negated and the force acting on the plate is only due to the liquid surface tension [13]:

$$F = 2\gamma t_p w_p \cos\theta \tag{3.3}$$

where t_p is the thickness of the plate, and w_p is the width of the plate. For this research, the plate consisted of a thin platinum strip which had been roughened so the contact angle between the liquid solution and the plate was zero (i.e. cos θ = 1). If this assumption holds

the surface tension can be determined directly from the measured force and the dimensions of the plate:

$$\gamma = \frac{F}{2t_p w_p} \tag{3.4}$$

In practice, the plate is suspended from a highly sensitive electro-balance by a thin wire and the liquid sample is raised until the surface just touches the hanging plate. The force measured by the electro-balance is used along with the dimensions of the plate, or in some cases a plate calibration factor, to calculate the surface tension. For dynamic studies the measurement is recorded at specific intervals until the force is no longer changing. The major disadvantage of the Wilhelmy plate technique is the relatively large quantity of sample required. For this reason, along with some sample environment control issues (discussed in Chapter 4), the Wilhelmy plate method was used as confirmation of the ADSA-P technique only.

In order to replicate the vapor phase conditions from the pendant drop experiments a custom sample cell had to be fabricated. A schematic of the cell is shown in Figure 3.2. The inner sample compartment, where the surface tension measurements were executed, is analogous to the pendant drop in the ADSA-P method. The separate outer compartment, designed for the addition of the environment solution to create the surrounding vapor phase, is analogous to the cuvette in the ADSA-P method. The force measurement was generated by a Langmuir-Blodgett Minitrough system from KSV Instruments, Ltd (Monroe, CT). All experiments were carried out at room temperature.

Before each run 5 ml of purified water was added to the inner sample cell and the plate was positioned so that the reading on the scale was approximately 72.6 mN/m. When the reading stabilized the balance was zeroed and the water was removed from the cell by aspiration. This gave the balance a zeroed reference relative to the surface tension of pure water. Next, 50 ml of sample solution was added to the outer compartment and the system was sealed with Parafilm. For consistency with the ADSA-P technique the vapor phase was allowed to equilibrate for 15 minutes, after which 5 ml of sample solution was added to the inner cell. Data collection was initiated immediately after the sample solution came in contact with the Wilhelmy plate and continued until equilibrium was reached and the measured force was no longer changing. After each use the glass sample cell was rinsed with ethanol and purified water, cleansed by ultrasonic, and dried.

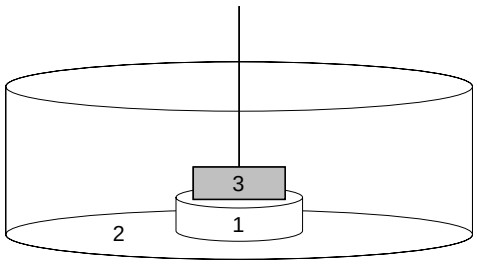

Figure 3.2: Schematic of the custom Wilhelmy plate sample cell; (1) inner sample compartment, (2) outer sample compartment, and (3) platinum Wilhelmy plate connected to the KSV electro-balance.

3.3 Contact Angle Measurements

The contact angle measurements were performed to illustrate a possible consequence of the observed surface tension phenomenon. The experiments were carried out using the ADSA-P method. In this technique the contact angle is determined based on the shape of an axisymmetric sessile drop formed on a solid surface. Similar to the pendant drop, surface tension forces tend to make the sessile drop spherical, whereas gravity tends to flatten the

drop [14]. The experimental profile of the sessile drop is fit to the theoretical Laplacian curve [Equation (3.1)] through a nonlinear regression routine. The objective function, which describes the deviation between the experimental sessile profile and the theoretical solution of the Laplace equation, is minimized using a combination of the Newton-Raphson and Levenberg-Marquardt methods. The contact angle and surface tension of the drop are generated as a result of the optimization [49, 52].

The shape of a liquid drop on a solid surface is dictated by the equilibrium between three interfacial tensions as illustrated in Figure 3.3 [52]. The equation describing this equilibrium and the relation to the liquid contact angle was first derived by Thomas Young in 1805, and thus, is referred to as Young's equation [13]:

$$\gamma_{lv} \cos\theta = \gamma_{sv} - \gamma_{sl} \tag{3.5}$$

where γ_{lv} is the liquid-vapor surface tension, γ_{sv} is the solid-vapor surface tension, γ_{sl} is the solid-liquid surface tension, and θ is the Young contact angle. The derivation of Young's equation assumes that the solid surface is smooth, homogeneous and rigid, and that it is chemically and physically inert with respect to the liquid being studied [52].

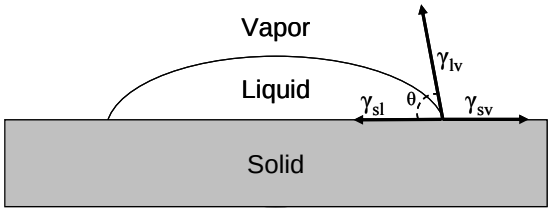

Figure 3.3: Schematic of the equilibrium between the interfacial tensions and the Young contact angle of a liquid sessile drop on a solid surface.

The experimental setup for the contact angle measurements was similar to the surface tension experiments (Figure 3.1A). The solid surface was placed inside the environmental chamber

and the sessile drop formed on top of the surface for image analysis. The substrate chosen for this study was cellulose acetate coverslips from Canemco & Marivac, Inc (Montreal, Quebec). Before each run a new coverslip was rinsed with ethanol and purified water, and dried with filtered air. After drying the fresh coverslip was fixed to the top of a Teflon base inside the chamber and approximately 10 ml of purified water was added to the bottom of the chamber to saturate the environment with water vapor. The chamber was then sealed with Parafilm and the vapor phase was allowed to equilibrate for 15 minutes. After equilibration 50 µl of sample solution was deposited on the coverslip with a micro-pipette through a small hole in the Parafilm. Data collection was initiated immediately after the sessile drop was formed and continued for approximately 3 hours, or until the contact angle was no longer changing.

Chapter 4

Experimental Study of Surfactant Adsorption

4.1 Introduction

The following chapter presents the experimental investigation portion of the research on surfactant adsorption of some selected surfactants at the vapor/liquid interface. The main focus is on dynamic surface tension measurements of aqueous solutions containing slightly volatile, organic amphiphiles. The majority of the experiments are carried out using the Axisymmetric Drop Shape Analysis-Profile (ADSA-P) technique due to the high accuracy and sample environment control capabilities of the method. An amphiphile is a chemical compound that possesses both hydrophobic (water hating) and hydrophilic (water loving) properties. The hydrophobic portion of the molecule usually includes a non-polar hydrocarbon chain ranging from 4 – 16 carbon atoms in length. The hydrophilic portion consists of a polar functional group attached to the hydrocarbon backbone. The functional group can be an alcohol (RCH_2OH), a fatty acid ($RCOOH$), a sulfate (RSO_4H), an amine (RNH_3^+), or any other polar group that gives the molecule hydrophilic properties. The amphiphilic nature of these molecules allows them to form interactions with adjacent water molecules through the formation of hydrogen bonds between the polar groups. These interactions increase the solubility of the compounds in water, which otherwise would be minimal due to the hydrophobic nature of the carbon chain.

The organization of the chapter is as follows. The dynamic surface tension experiments on the organic compounds by the ADSA-P method are presented in Section 4.2 along with some

traditional surfactants for comparison. To verify the data, select cases were repeated using the Wilhelmy plate method. These results are presented in Section 4.3. In Section 4.4 the surface tension response to a change in drop volume is examined. Further confirmation of the ADSA-P results was obtained indirectly by studying the time-dependent contact angle as shown in Section 4.5. A summary of the experimental results is given in Section 4.6.

4.2 Dynamic Surface Tension by ADSA-P

The following section outlines the Dynamic Surface Tension (DST) results by the ADSA-P method. The results are organized into three subsections according to the various surfactants studied. Data from the aqueous alcohols are presented in the first subsection followed by some additional amphiphiles to emphasize the similarities within this class of organic molecules. In the final subsection, results from some traditional surfactants are displayed to illustrate the differences from the organic amphiphiles.

The experimental procedure for the surface tension experiments is outlined in detail in Chapter 3. Briefly, a pendant drop of the sample under test (drop solution) was formed inside a clear quartz cuvette above 1 ml of aqueous solution containing the same component as in the drop (environment solution). If the two liquid solutions had different surfactant concentrations, a driving force was established for molecular transfer across the vapor/liquid interface causing the surface tension of the drop solution to evolve as a result of the exchange. Three distinct concentration-difference conditions were explored: positive when the drop solution concentration was greater than the environment solution concentration, negative when the drop concentration was less than the environment concentration, and zero

when the two were equal. For each surfactant a range of concentrations was prepared to facilitate a number of variations of the three concentration difference conditions.

4.2.1 Aqueous n-Alcohols

1-Octanol: The first compound studied in this research was 1-octanol; a straight chain hydrocarbon with a small polar group attached at the first carbon (C1) position. The time-dependent or Dynamic Surface Tension (DST) profiles for the aqueous 1-octanol system, at six different environment solution concentrations, are shown in Figure 4.1. Each profile begins with an initial induction phase approximately 10 to 100 seconds in length, followed by an increase or decrease in surface tension toward a final steady-state or "equilibrium". In each case, the overall trend, or the rate of change, of the surface tension seems to be controlled by the concentration difference between the vapor phase, exerted by the environment solution, and the drop solution. For the positive concentration difference cases the surface tension increases as surfactant desorbs from the interface into the vapor phase. For the negative concentration difference cases the surface tension decreases as surfactant adsorbs at the interface from the vapor phase. Finally, for the zero concentration difference cases the surface tension remains essentially constant as there is no driving force for molecular transfer. The surface tension continues to change until a final steady-state is reached between the interface and the two bulk phases (liquid and vapor).

Interestingly, for each environment solution concentration, a similar final, constant surface tension value is attained by each profile regardless of the concentration of the drop solution. In Figure 4.1A, where the environment solution is pure water, each profile converged towards a surface tension of approximately 70 mN/m, which is very close to the surface

tension of pure water. Similar results were also observed for the other five environment solutions. In each case the final, constant surface tension is similar to the surface tension of the environment solution. This suggests that at the final steady-state conditions the surface tension is determined primarily by the concentration of the environment solution. This is in contrast to traditional surfactants where the surface tension is largely dependent on the concentration of the bulk liquid phase. From these results it can be presumed that initially the surface tension is controlled by a combination of adsorption from the liquid and the vapor phase, whereas at the final steady-state the surface tension is determined primarily by adsorption from the vapor phase. Confirmation of these observations was obtained through theoretical modeling, and will be discussed in detail in Chapter 5.

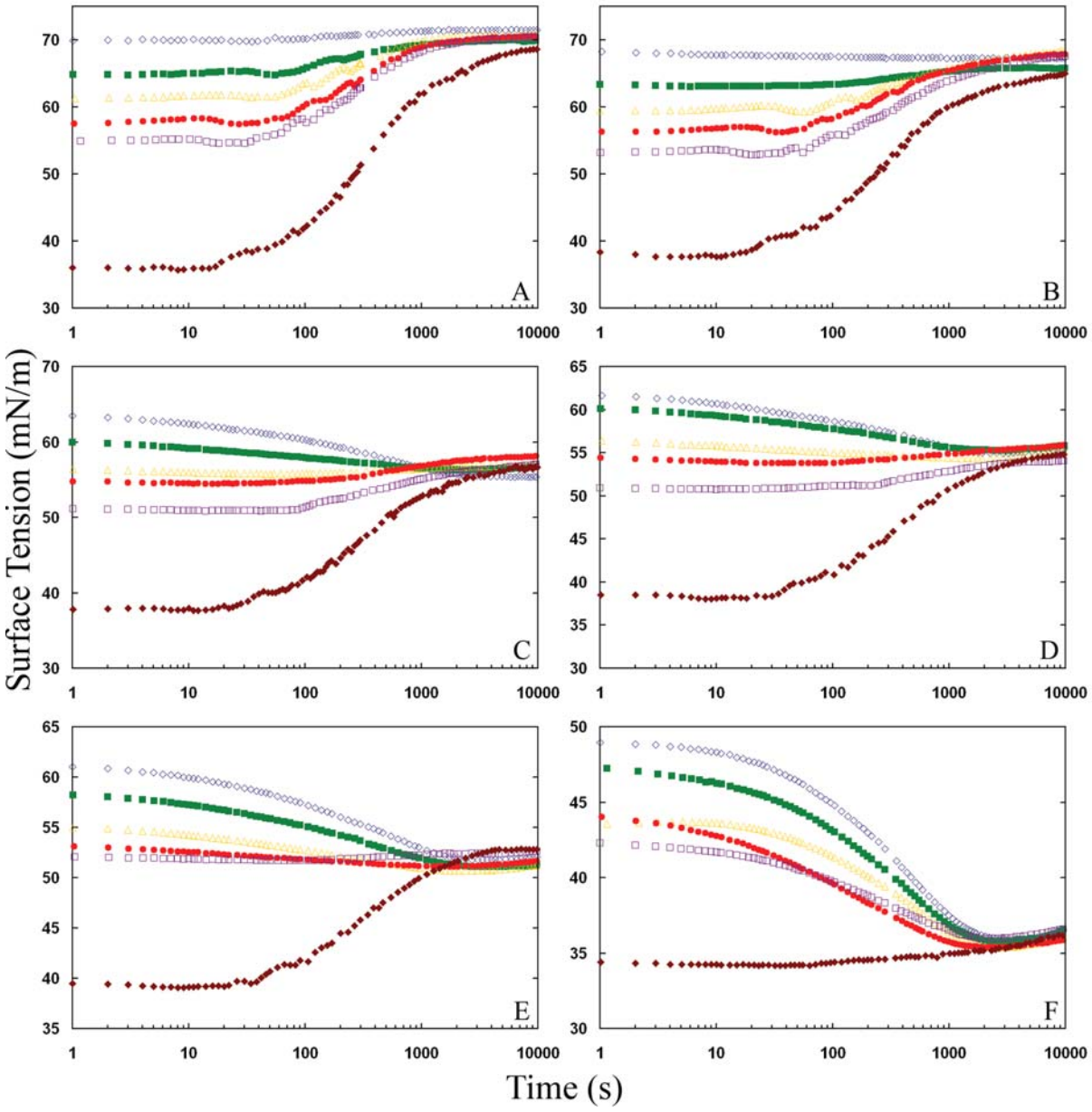

Figure 4.1: Aqueous 1-octanol dynamic surface tension profiles for drop solution concentrations of 0.2 mol/m^3 (◊), 0.4 mol/m^3 (■), 0.6 mol/m^3 (△), 0.8 mol/m^3 (●), 1.0 mol/m^3 (□), and 2.92 mol/m^3 (♦). Each graph represents a different environment solution concentration; (A) pure water, (B) 0.2 mol/m^3, (C) 0.6 mol/m^3, (D) 0.8 mol/m^3, (E) 1.0 mol/m^3, and (F) 2.92 mol/m^3.

1-Hexanol: To determine if these distinctive results were limited to the 1-octanol system, aqueous solutions of 1-hexanol were also investigated. As seen in Table 3.1 hexanol is more soluble in water and has a higher volatility than octanol due to the shorter carbon chain.

However, the two are extremely similar in terms of structure and it is expected that the results should also be quite similar. The DST profiles for the aqueous 1-hexanol system, at four different environment solution concentrations, are shown in Figure 4.2. As expected the results are very similar to the 1-octanol system. As each experiment proceeds, the rate of change of the surface tension and the direction seems to be controlled by the concentration difference between the vapor phase and the drop solution, following the same trend that was observed with the 1-octanol solutions. Furthermore, for each environment solution concentration, a similar final, constant surface tension value is attained by each profile regardless of the concentration of the drop solution. As with octanol, the final steady-state surface tension corresponds closely to the surface tension of the environment solution. Once again, these results imply that adsorption from the vapor phase has a significant influence on the surface tension, particularly at the final steady-state where it seems to be the primary factor. The results also demonstrate that the observed phenomenon is not limited to 1-octanol, but may be general to this class of organic compounds.

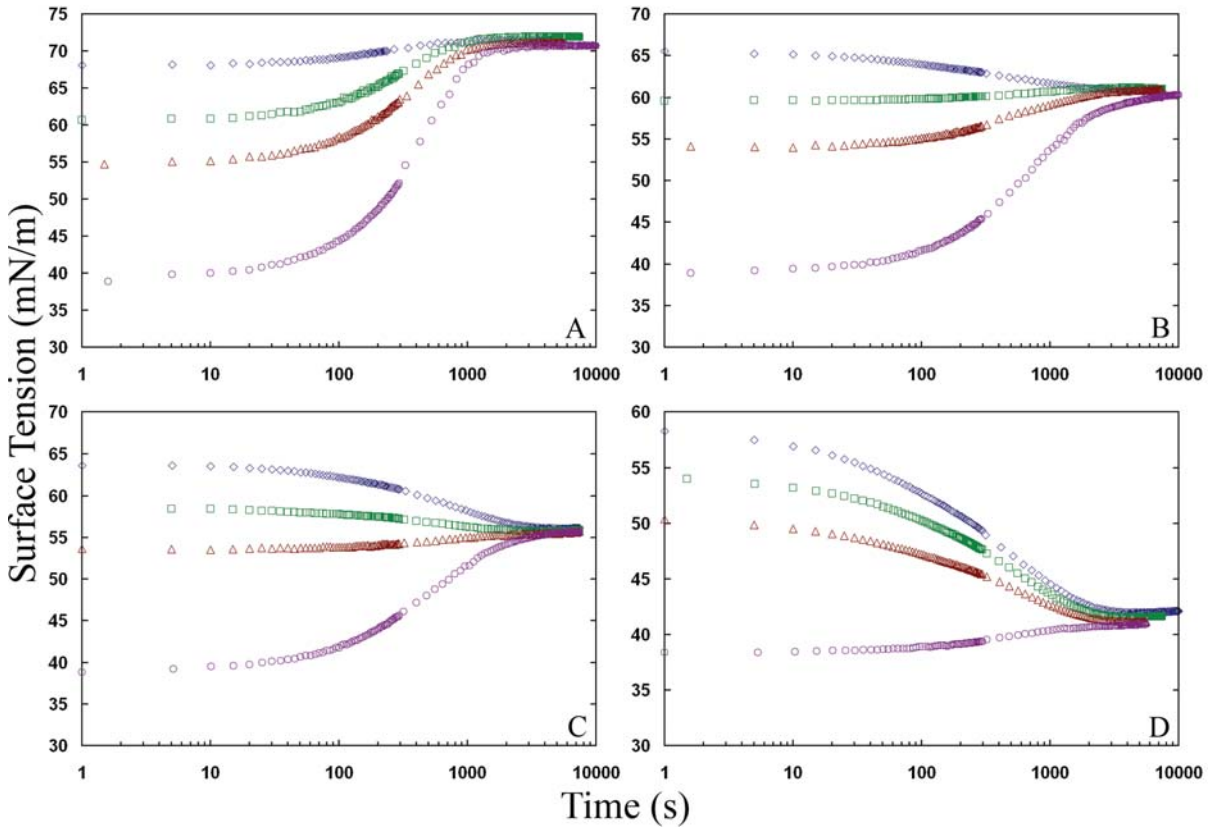

Figure 4.2: Aqueous 1-hexanol dynamic surface tension profiles for drop solution concentrations of 2 mol/m^3 (◊), 5 mol/m^3 (□), 9 mol/m^3 (△), and 30 mol/m^3 (○). Each graph represents a different environment solution concentration; (A) pure water, (B) 5 mol/m^3, (C) 9 mol/m3, and (D) 30 mol/m^3.

1-Butanol: The next compound was chosen to investigate the effect of the carbon chain length on the observed results. Similar to 1-octanol, 1-butanol is a straight chain hydrocarbon with a small polar group attached at the C1 position. However, butanol is four carbons shorter than octanol giving it a much higher volatility and solubility in water (Table 3.1). The DST profiles for the aqueous 1-butanol system, at four different environment solution concentrations, are shown in Figure 4.3. The results from butanol are very similar to both octanol and hexanol. This suggests that in-between octanol and butanol there is no effect of the increased solubility and volatility on the surface tension results due to shortening the carbon chain length. Furthermore, the observed phenomenon seems to be rather general in

nature a may be related to the molecular structure and physical properties shared by this class of organics.

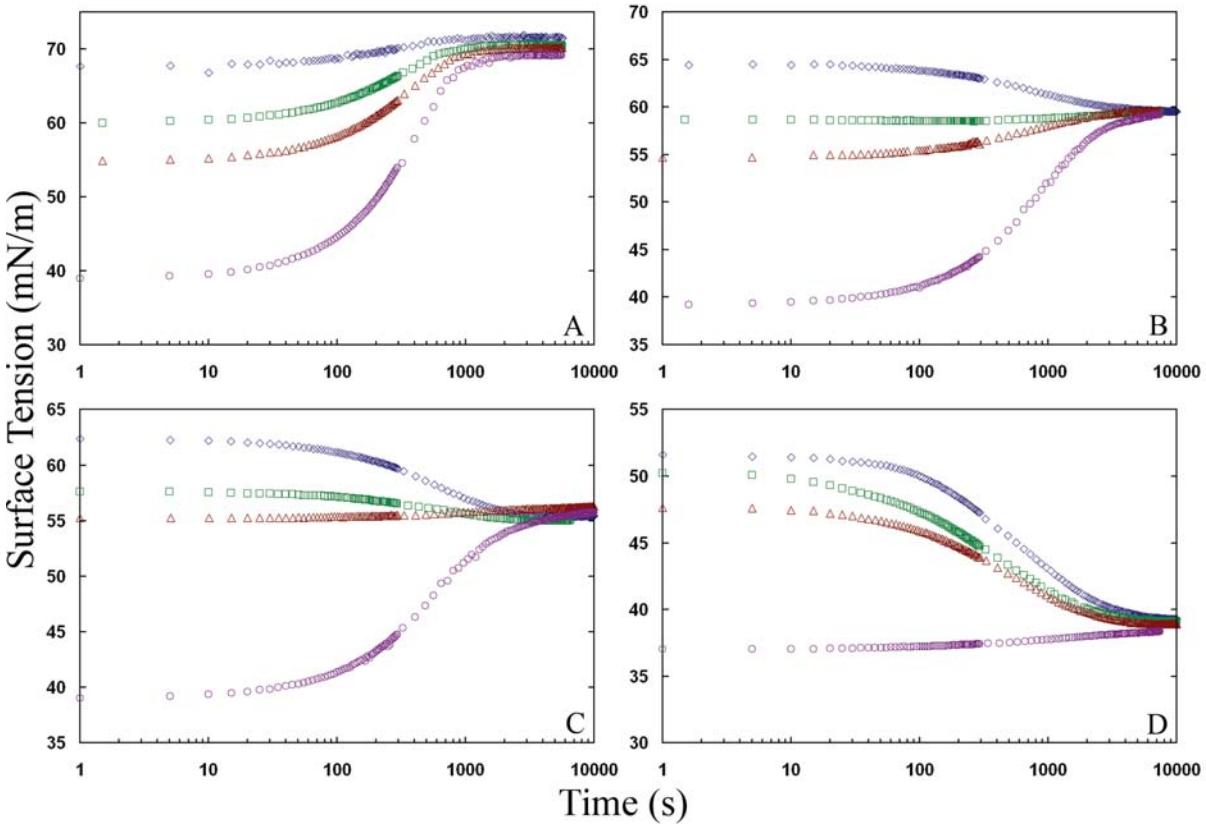

Figure 4.3: Aqueous 1-butanol dynamic surface tension profiles for drop solution concentrations of 20 mol/m^3 (◊), 60 mol/m^3 (□), 100 mol/m^3 (△), and 400 mol/m^3 (○). Each graph represents a different environment solution concentration; (A) pure water, (B) 60 mol/m^3, (C) 100 mol/m^3, and (D) 400 mol/m^3.

1-Decanol: The next compound was chosen to investigate the effect of increasing the carbon chain length on the surface tension results. Decanol is two carbons longer than octanol which reduces the water solubility and volatility considerably (Table 3.1). Increasing the carbon chain length any further lowers the solubility to the point where solution preparation becomes difficult. Decanol has also been reported to be a slower diffusing molecule compared to shorter chain alcohols due to the length of its hydrocarbon chain [18, 24]. It is expected that this may also influence the surface tension results. The DST profiles for the

aqueous 1-decanol system, at four different environment solution concentrations, are shown in Figure 4.4. The results from 1-decanol are quite different compared to the previous three systems. Because decanol is a slower diffusing molecule it seems that initially there are signs of mixed diffusion and transfer effects until the concentration at the interface is established. This would explain why the initial surface tension values are closer to water surface tension (72 mN/m) than the previous systems, especially for the cases where the drop concentration is high, and why the surface tension decreases initially for the positive concentration difference cases. Once the surfactant begins to accumulate at the interface, transfer takes over and the surface tension trends toward the final steady-state value. As with the previous systems, the final steady-state surface tension attained by each profile is similar for each environment, regardless of the concentration of the drop solution. The diffusion effect can be observed in the surface tension data at the onset of the experiments until the concentration at the interface is fully established. Another explanation for the difference in the results when increasing the carbon chain length could be the subsequent increase in hydrophobicity of the surfactant. The longer hydrocarbon chain makes the molecule more hydrophobic as illustrated by the decrease in solubility compared to the shorter alcohols. The increase in hydrophobicity, coupled with the length of the molecule, may slow the arrangement of the surfactants at the interface and affect the measured surface tension. The results from decanol illustrate that increasing the length of the carbon chain does have an influence on the adsorption of surfactant to the interface. However, the chain length effect was only evident for the longest compound studied; the results from the shorter alcohols showed no influence of hydrocarbon chain length.

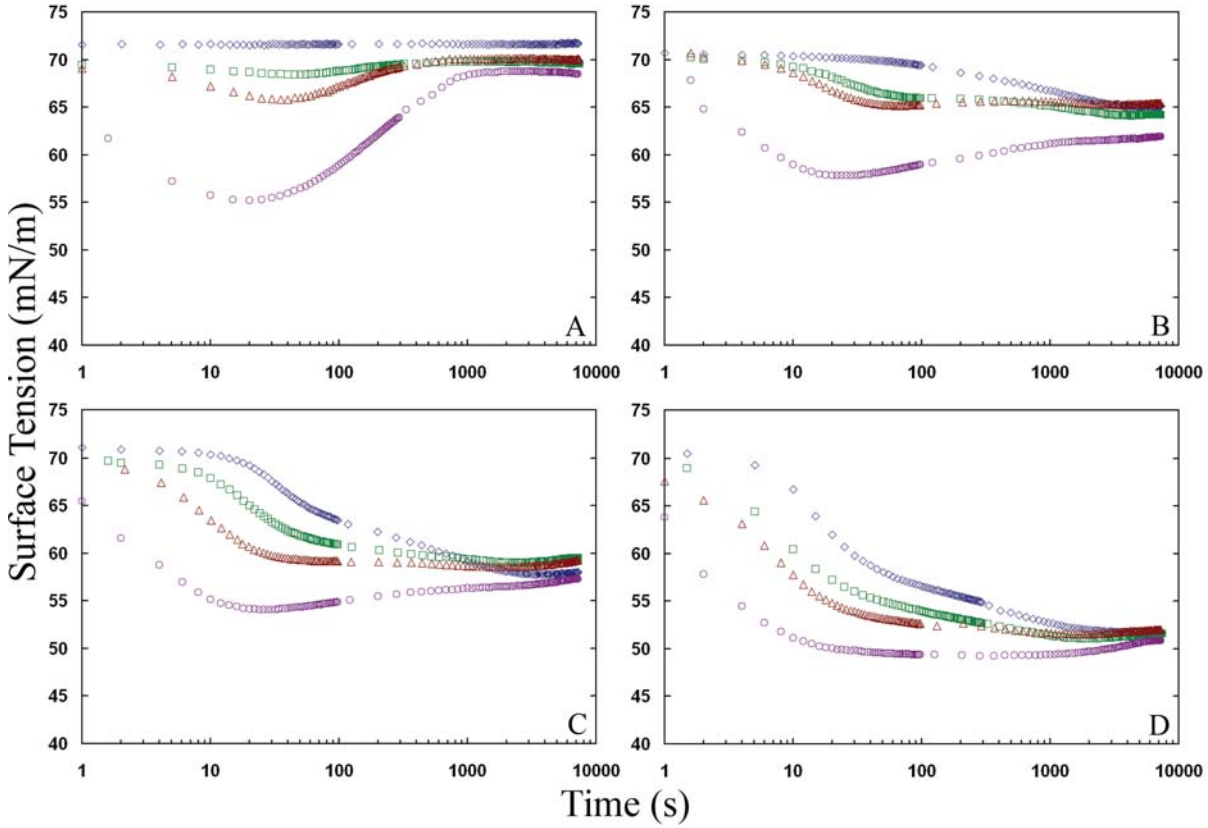

Figure 4.4: Aqueous 1-decanol dynamic surface tension profiles for drop solution concentrations of 0.02 mol/m^3 (◊), 0.05 mol/m^3 (□), 0.08 mol/m^3 (△), and 0.15 mol/m^3 (○). Each graph represents a different environment solution concentration; (A) pure water, (B) 0.05 mol/m^3, (C) 0.08 mol/m3, and (D) 0.15 mol/m^3.

4.2.2 Other Amphiphiles

The observed phenomenon has been demonstrated to be comparable for a number of different alcohols with similar structures and a range of carbon chain lengths. The next step was to investigate other amphiphiles to determine if the results were limited to alcohol molecules only. The compounds were chosen to have structures similar to octanol with the only difference being the functional group attached to the hydrocarbon chain.

1-Octanoic Acid: The first compound chosen to investigate the effect of changing the functional group on the carbon chain was 1-octanoic acid, which is a straight chain hydrocarbon with a carboxyl group attached at the C1 position. The solubility of octanoic acid is very similar to octanol; however, the vapor pressure is one order of magnitude lower at 25°C (Table 3.1). The DST profiles for the aqueous 1-octanoic acid system, at three different environment solution concentrations, are shown in Figure 4.5. The results are quite similar to octanol and the other alcohols in general, with the exception of decanol. Once again, the overall trend in the surface tension seems to be controlled by the concentration difference across the interface and the final steady-state surface tension values attained for each profile are comparable when the environment solution concentration is held constant. One notable difference is the time-scale for equilibration. For the 1-octanol system the final steady-state was reached within approximately 3 hours, whereas for the 1-octanoic acid system it took anywhere from 6 to 14 hours. The disparity may be attributed to the difference in polarity of the molecules related to the two different functional groups. Also, the lower volatility compared to octanol may increase the time for equilibrium by slowing down the transfer across the vapor/liquid interface. The results for the 1-octanoic acid system prove that the observed phenomenon is not limited to alcohol molecules and may be general to any water soluble, organic amphiphile with non-trivial volatility.

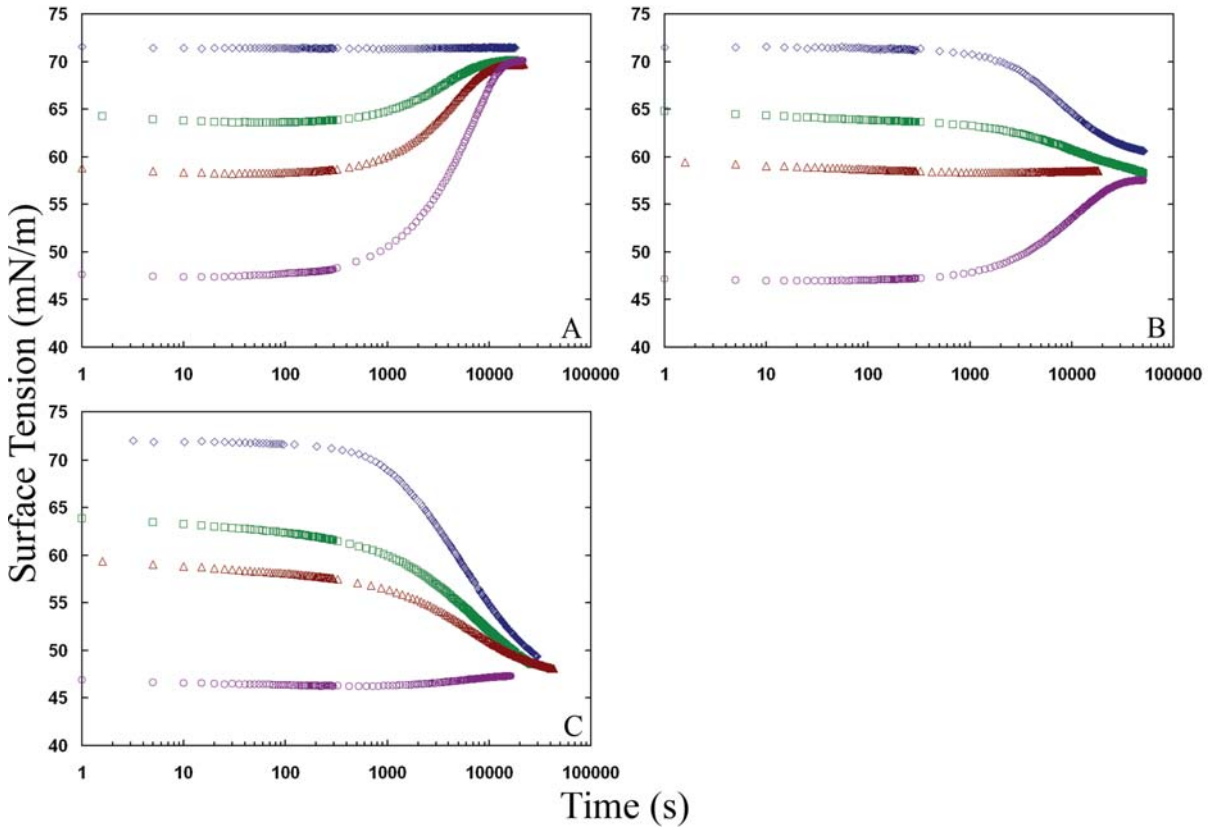

Figure 4.5: Aqueous 1-octanoic acid dynamic surface tension profiles for drop solution concentrations of 0.2 mol/m^3 (◊), 0.5 mol/m^3 (□), 0.8 mol/m^3 (△), and 2.0 mol/m^3 (○). Each graph represents a different environment solution concentration; (A) Pure water, (B) 0.8 mol/m^3, and (C) 2.0 mol/m^3.

1-Octylamine: The next compound chosen to investigate the effect of changing the functional group on the carbon chain was 1-octylamine, which is a straight chain hydrocarbon with an amine group at the C1 position. The increased polarity of the amine group increases the solubility of octylamine in water considerably compared to octanol (Table 3.1). The DST profiles for the aqueous 1-octylamine system, at four different environment solution concentrations, are shown in Figure 4.6. The results for octylamine are similar to octanol for the cases when the environment solution is either pure water (Figure 4.6A) or very concentrated (Figure 4.6D). However, when the environment solution is of intermediate concentration (Figure 4.6B and Figure 4.6C) the results are similar to the pure

water case. It seems that below a certain concentration the vapor phase has no influence on the adsorption, and the surface tension behaves as though the surrounding environment is saturated with water vapor. The only distinction between these systems is the functional group attached to the hydrocarbon chain. Thus, the discrepancy in the surface tension trend must be attributed to the difference in polarity between the hydroxyl group and the amine group.

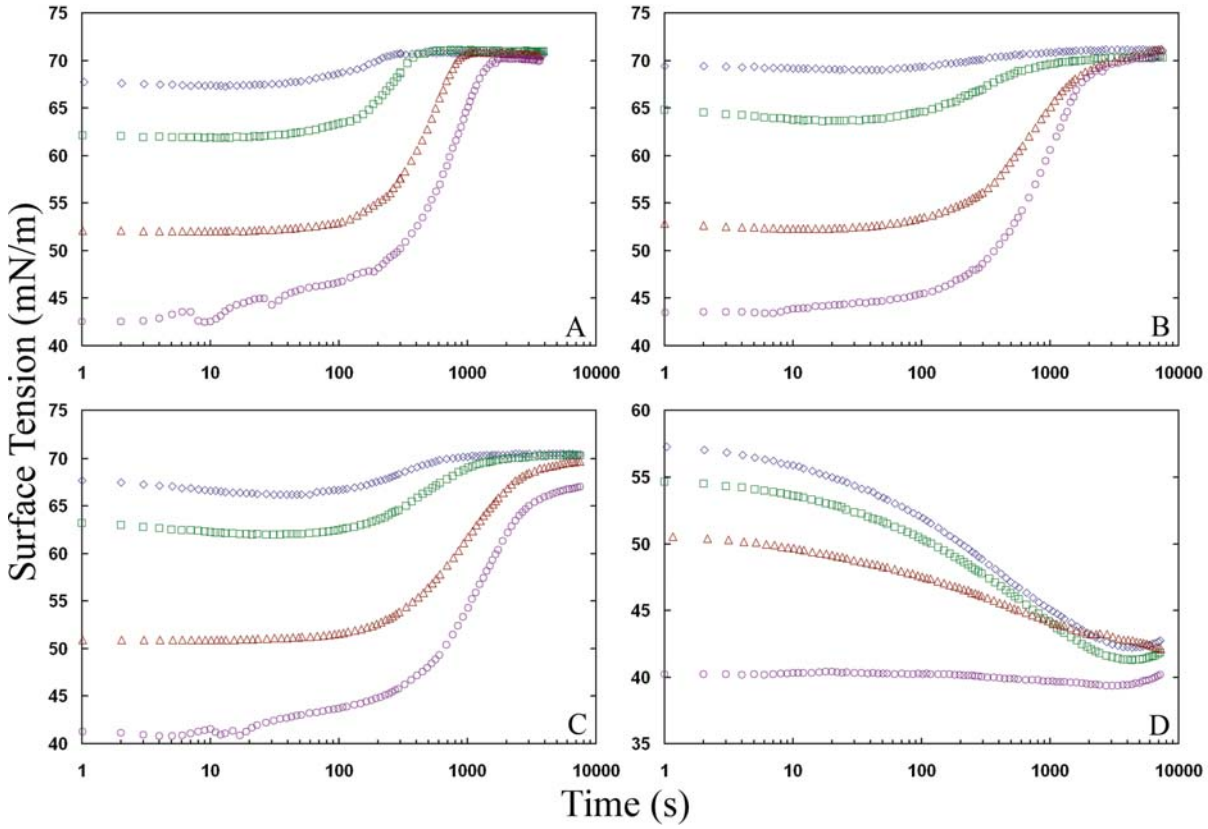

Figure 4.6: Aqueous 1-octylamine dynamic surface tension profiles for drop solution concentrations of 0.5 mol/m^3 (◊), 0.9 mol/m^3 (□), 2.0 mol/m^3 (△), and 4.0 mol/m^3 (○). Each graph represents a different environment solution concentration; (A) pure water, (B) 0.5 mol/m^3, (C) 0.9 mol/m3, and (D) 4.0 mol/m^3.

4.2.3 Traditional Surfactants

In the following section the results from two traditional surfactant systems are presented to illustrate the differences between these systems and the organic amphiphiles presented in the previous two sections. Two groups of nonionic surfactants that are commonly used in industrial applications include polyoxyethylene alcohols (C_mE_n) and polyoxyethylene alkylphenols. One representative surfactant was chosen from each group for investigation in this research; octaethylene glycol mono-n-dodecyl ether ($C_{12}E_8$) from the alcohols and polyoxyethylene (12) nonyl phenyl ether (Igepal-CO-720) from the alkylphenols. The DST profiles for the aqueous solutions of $C_{12}E_8$ and Igepal-CO-720 at various drop solution concentrations are shown in Figure 4.7 and Figure 4.8, respectively. In both cases the environment solution is pure water. For these surfactants the surface tension is mainly a function of the concentration of the drop solution and independent of the vapor phase, particularly at the final steady-state where each profile reaches a distinct equilibrium surface tension. Contrast this with the organic amphiphiles where the final steady-state surface tension is controlled by the vapor phase and independent of the drop solution concentration.

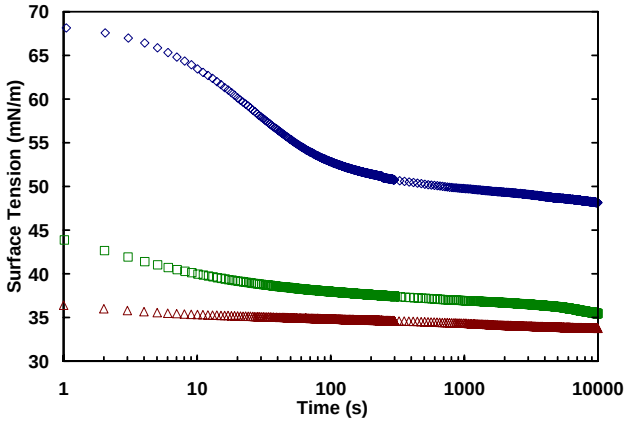

Figure 4.7: Aqueous octaethylene glycol monododecyl ether ($C_{12}E_8$) dynamic surface tension profiles for drop solution concentrations of 0.008 mol/m^3 (◊), 0.04 mol/m^3 (□), and 0.093 mol/m^3 (△). Environment solution is pure water.

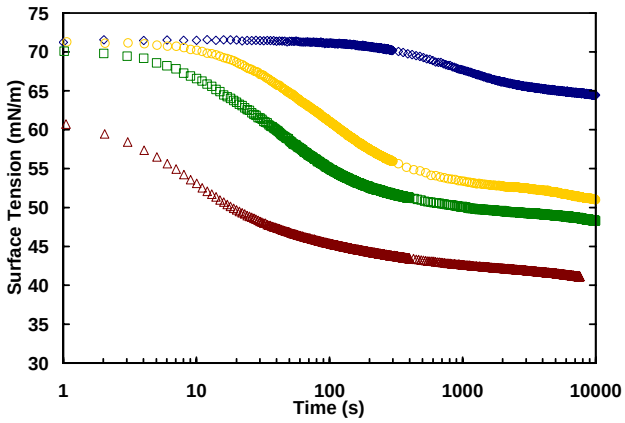

Figure 4.8: Aqueous Igepal CO-720 dynamic surface tension profiles for drop concentrations of 0.00123 mol/m^3 (◊), 0.00657 mol/m^3 (○), 0.00985 mol/m^3 (□), 0.0246 mol/m^3 (△) [31]. Environment solution is pure water.

4.3 Dynamic Surface Tension by the Wilhelmy Plate Method

The following section outlines the Dynamic Surface Tension (DST) results by the Wilhelmy plate method. The purpose of these experiments was to provide confirmation of the surface tension results obtained by the ADSA-P method. The two compounds chosen for the verification were 1-octanol and 1-butanol. The solutions were prepared at the same concentrations as the ADSA-P experiments to provide a direct comparison between the two methods. Due to certain limitations associated with the Wilhelmy plate technique, discussed below, it is expected that there will be differences in the absolute surface tension values measured by the two methods. However, the main objective of these experiments is to determine if the overall trend in the surface tension can be reproduced.

4.3.1 1-Octanol

The DST profiles for the aqueous 1-octanol system by the Wilhelmy plate method, at four different environment solution concentrations, are shown in Figure 4.9. When comparing these results to the data from the ADSA-P method in Figure 4.1 a number of differences are

immediately evident. First, the time-scale for equilibration is much longer for the Wilhelmy plate method. This is due to the increased volume and exposed surface area of the system compared to ADSA-P. For the Wilhelmy plate the volumes of the sample under test and environment solution are 5 ml and 50 ml, respectively, whereas for ADSA-P the pendant drop volume is approximately 0.02 ml and the environment solution is 1 ml. Thus, the extended time-scale is expected. Second, the specific value of the surface tension at a given time and concentration may be quite different between the two methods due mainly to limitations of the Wilhelmy plate technique. The sample cell used in this study was designed to recreate the unique vapor phase conditions inside the environmental chamber during the ADSA-P experiments. The system is sealed with Parafilm but a small hole has to be left in the center of the film to allow the wire from the electro-balance connected to the Wilhelmy plate to enter the cell. The balance has a very high sensitivity and it is crucial that nothing touch the wire during measurement. Thus, during the experiment it is possible for the volatile surfactant to escape from the system through the hole in the Parafilm. This would influence the surface tension values since the component is constantly being depleted from the system. Despite these discrepancies the main objective of the experiments was achieved since in each case the overall trend of the surface tension profiles was reproduced by the Wilhelmy plate method. The fact that comparable data was generated by two methods based on different measurement principles proves the results are not a product of the method used and increases the confidence in the ADSA-P surface tension results.

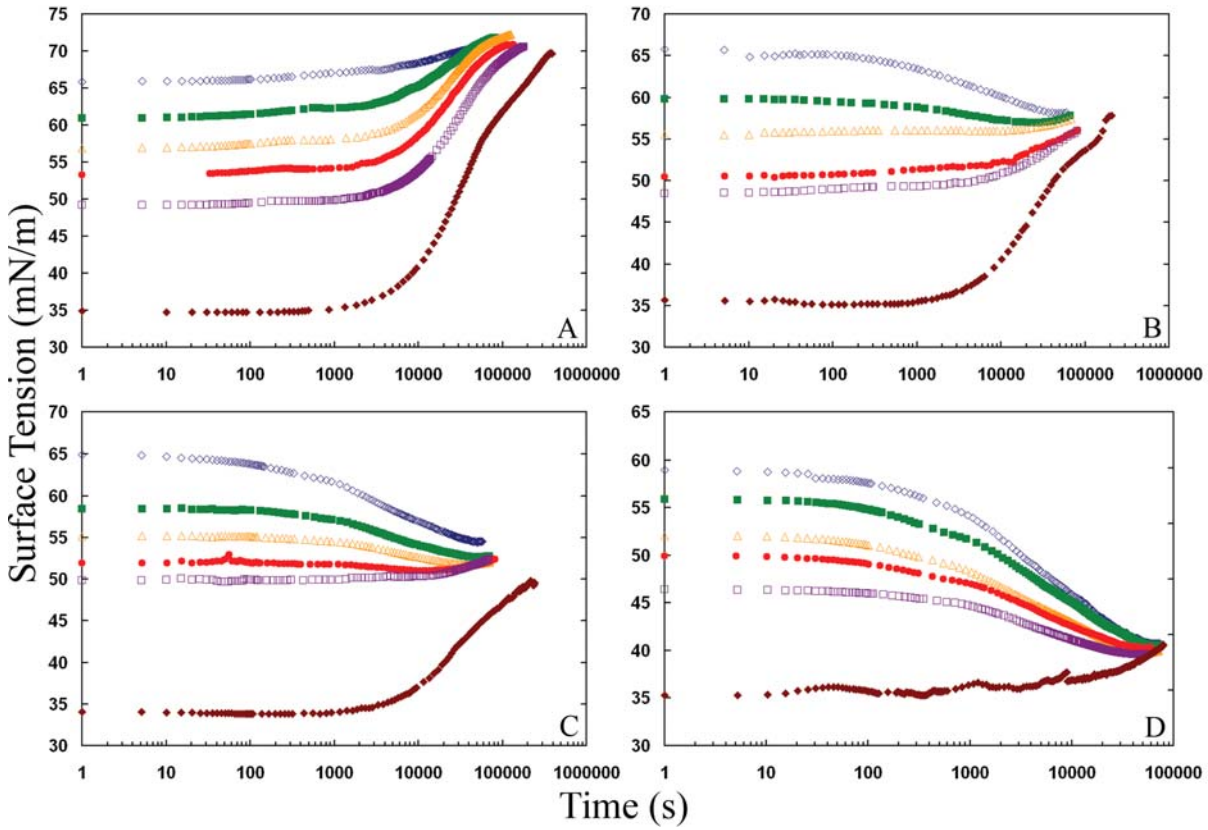

Figure 4.9: Aqueous 1-octanol dynamic surface tension profiles by the Wilhelmy plate method for drop solution concentrations of 0.2 mol/m^3 (◊), 0.4 mol/m^3 (■), 0.6 mol/m^3 (△), 0.8 mol/m^3 (●), 1.0 mol/m^3 (□), and 2.92 mol/m^3 (♦). Each graph represents a different environment solution concentration; (A) pure water, (B) 0.6 mol/m^3, (C) 1.0 mol/m^3, and (D) 2.92 mol/m^3.

4.3.2 1-Butanol

The DST profiles for the aqueous 1-butanol system by the Wilhelmy plate method, at four different environment solution concentrations, are shown in Figure 4.10. The corresponding data from the ADSA-P method is shown in Figure 4.3. The differences in the results of the two methods are similar to those that were observed for the 1-octanol system. Once again, the specific value of the surface tension at a given time and concentration measured by the Wilhelmy plate may be different than the corresponding ADSA-P data. However, the inconsistency is less evident for butanol, especially at the lower environment solution concentrations. For the highest environment solution concentration (Figure 4.10D) the initial surface tension is consistently higher when compared to the ADSA-P results. This may be

caused by the increased volatility of the butanol system. The vapor phase is allowed to equilibrate for 15 minutes before the solution under test is added to the cell and the experiment begins. During this time the volatile component can escape from the system since the cell cannot be completely sealed. Thus, when the experiment starts the concentration of the environment solution will be slightly depleted causing the surface tension to be higher than expected. This also explains why the surface tension increases over time for the zero concentration difference case ($C_{drop} = C_{env}$) in Figure 4.10D. From the ADSA-P results it is expected that this profile should be essentially constant over the duration of the experiment. However, if surfactant from the environment solution has leaked out of the system, when the experiment begins the concentration of the drop solution will be higher than the concentration of the environment solution and the surface tension will increase before reaching a final steady-state value. Despite the differences between the two methods the main objective was to replicate the overall trend in the surface tension results from the ADSA-P technique, which again was accomplished successfully. This further increases the confidence in the ADSA-P surface tension results.

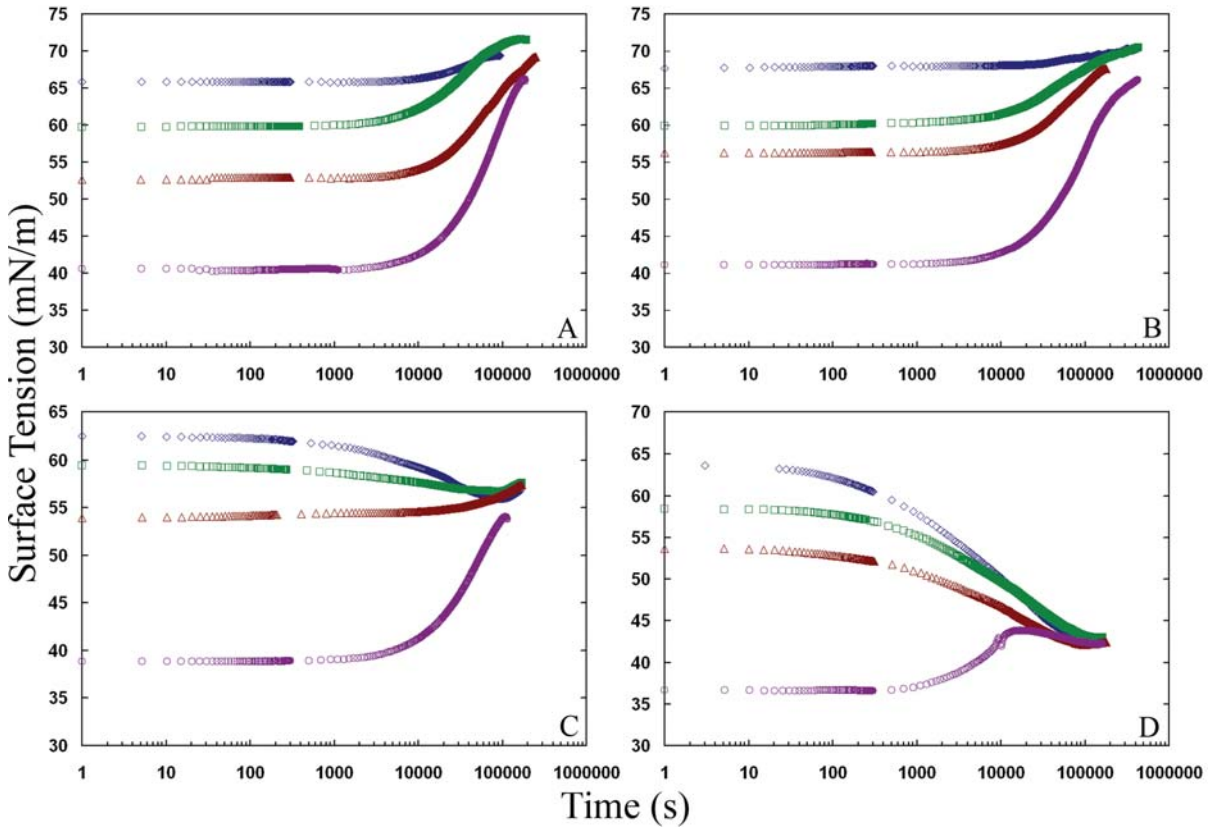

Figure 4.10: Aqueous 1-butanol dynamic surface tension profiles by the Wilhelmy plate method for drop solution concentrations of 20 mol/m^3 (◊), 60 mol/m^3 (□), 100 mol/m^3 (△), and 400 mol/m^3 (○). Each graph represents a different environment solution concentration; (A) pure water, (B) 20 mol/m^3, (C) 100 mol/m^3, and (D) 400 mol/m^3.

4.4 Surface Tension Response to a Change in Drop Volume

To further understand the behavior of the interface at the final steady-state conditions, several cases of the 1-octanol system were subjected to a sudden change in drop volume to disrupt the liquid interfacial structure. After the experimental "equilibrium" was attained, the pendant drop was either compressed or expanded using the motorized syringe pump and the effect on the interface was studied through the continuous measurement of surface tension. The results are shown in Figure 4.11. For the expansion experiments (open symbols), only the positive concentration-difference cases (i.e., drop solution concentration greater than environment solution concentration) showed any response to the volume change. For these

experiments, the surface tension exhibited a rapid decrease, followed by a gradual increase back to the "equilibrium" value prior to expansion. When the drop is expanded the barrier at the interface may be disrupted as fresh solution from the bulk is forced to the surface, causing the sudden decrease in surface tension due to the increase in surfactant concentration at the interface from the liquid phase. The negative concentration-difference expansions (i.e., drop solution concentration less than environment solution concentration) did not show any response to the volume increase. Since the final steady-state surface tension is dominated by the vapor phase, the lower concentration of the liquid phase may not be sufficient to cause a change in surface tension after the expansion. For the compression experiments (closed symbols), no response to the change in volume was observed regardless of the concentration of the drop or environment solutions. It is noted that the drop volume induced surface tension responses observed here are contradictory to results obtained with conventional surfactants, where an expansion in surface area is typically followed by a sudden increase in surface tension and a compression followed by a sudden decrease [53].

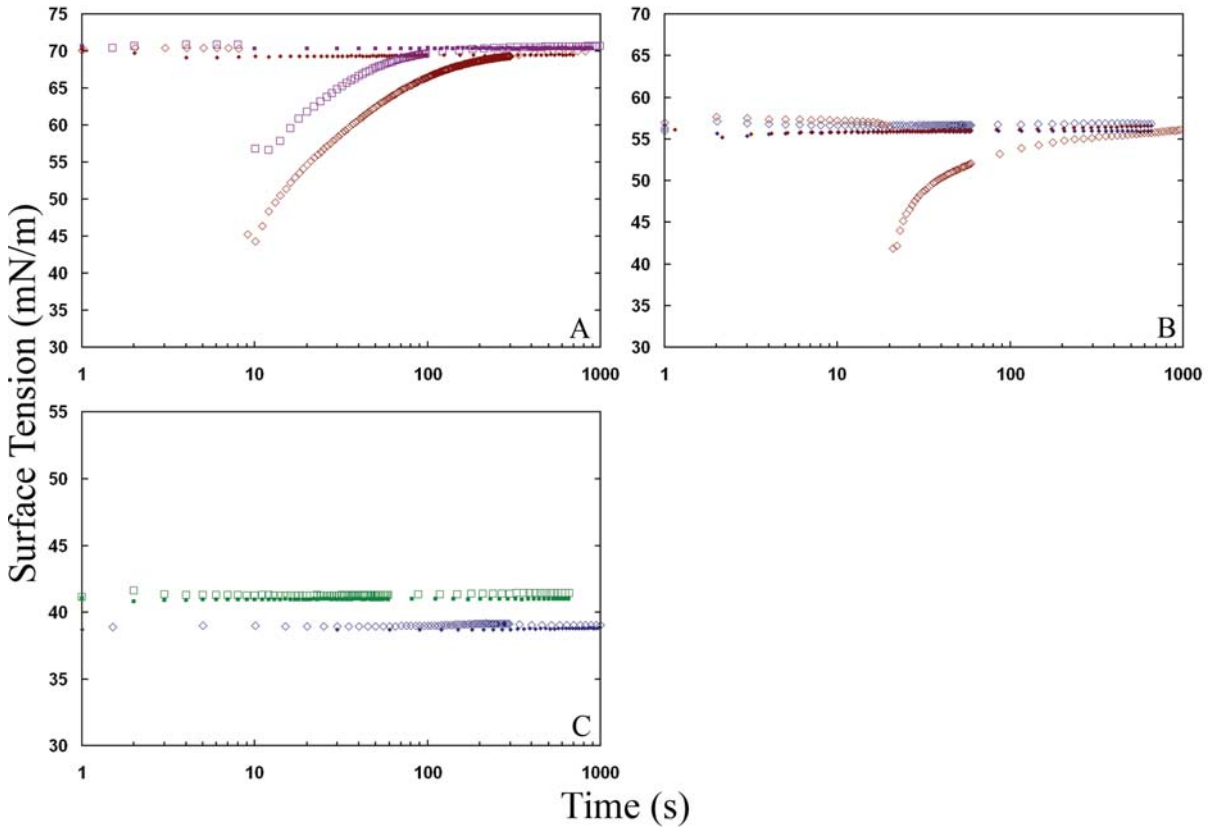

Figure 4.11: Aqueous 1-octanol surface tension response to a change in drop volume for drop solution concentrations of 0.2 mol/m^3 (◊, ♦), 0.4 mol/m^3 (□, ■), 1.0 mol/m^3 (□, ■), and 2.92 mol/m^3 (◊, ♦). Each graph represents a different environment solution concentration; (A) pure water, (B) 0.8 mol/m^3, and (C) 2.92 mol/m^3. Open symbols represent volume expansion and closed symbols represent volume compression.

Several 1-octanol solutions were also subjected to a saw-tooth pattern drop volume change to investigate the effect on the steady-state interfacial conditions. After the experimental "equilibrium" was attained, the pendant drop was expanded and then compressed in a continuous linear pattern using the programmable option of the motorized syringe pump. The effect on the interface was studied through the continuous measurement of surface tension. The drop volume change was set for 100 steps or 0.003 cm^3 in each direction and the cycle time was set at 300 seconds. The results are shown in Figure 4.12 and are very similar for each concentration. During the expansion the surface tension undergoes a sudden decrease,

followed by a gradual increase during the compression stage. The surface tension response during the expansion stage is delayed for a short period as the drop volume begins to increase. The response is more prominent for the higher drop concentrations and in each case the response is progressively diminished for each subsequent cycle. These results are as expected from the single compression/expansion experiments in Figure 4.11. The major response occurs during the expansion stage where the surface tension exhibits the abrupt decrease. The surface tension begins to recover toward the end of the expansion phase and into the compression stage. As with the single compression experiments no significant change in surface tension is detected as the drop volume decreases. A slight volume effect is observed in the surface tension response for the two lower drop solution concentrations. The surface tension decreases slightly as the drop is compressed and increases slightly as the drop is expanded before the sudden decrease occurs.

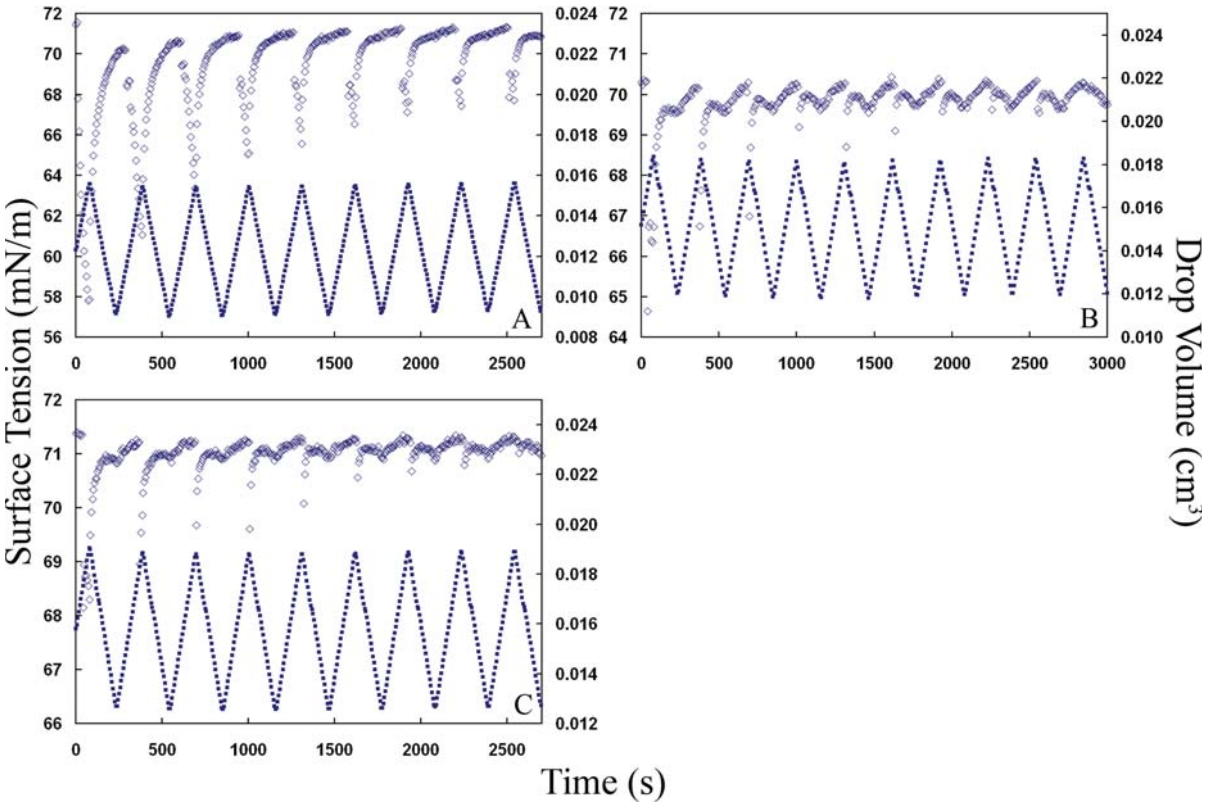

Figure 4.12: Aqueous 1-octanol surface tension response (◊) to a saw-tooth pattern drop volume change (■) for drop solution concentrations of 2.92 mol/m^3 (A), 1.0 mol/m^3 (B), and 0.8 mol/m^3 (C). Environment solution is pure water in all cases.

4.5 Time-Dependent Contact Angle Measurements

To illustrate a possible consequence of the observed surface tension phenomenon, time-dependent contact angle experiments were carried out on the aqueous 1-octanol solutions using the ADSA-P technique. The contact angle of a liquid solution on a solid surface is a widely used measure for industrial applications involving spreading and wetting [54]. The relation between the contact angle of a liquid drop and the surface tension of the drop is given by Young's equation [Equation (3.5)]. If changes in the solid-state interfacial tensions are negligible for a given solid surface, then any change in the liquid surface tension must be manifested in the contact angle. The experiments were performed on a cellulose acetate coverslip with pure water added to the bottom of the chamber to simulate the vapor phase

conditions from Figure 4.1A. Thus, for this specific case the contact angle should increase over time to reflect the increase in surface tension of the solution. The time-dependent contact angle results for the 1-octanol solutions are shown in Figure 4.13.

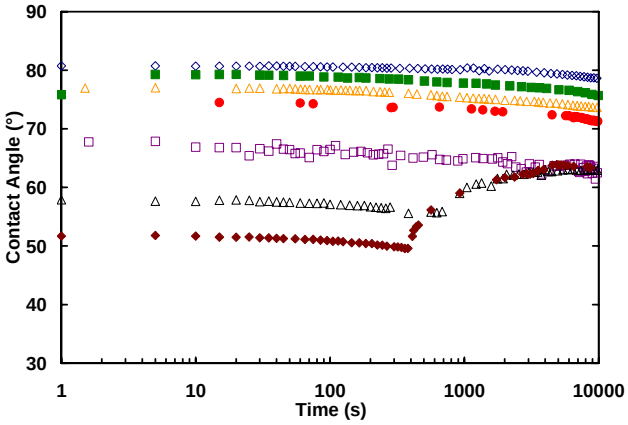

Figure 4.13: Aqueous 1-octanol time-dependent contact angle for drop solution concentrations of 0.2 mol/m^3 (◊), 0.4 mol/m^3 (■), 0.6 mol/m^3 (Δ), 0.8 mol/m^3 (●), 1.0 mol/m^3 (□), 2.0 mol/m^3 (Δ), and 2.92 mol/m^3 (♦). Environment solution is pure water.

Of the seven solutions prepared, only the two with the highest octanol concentrations showed the expected increase in contact angle. The contact angle of the other five solutions remained essentially constant over the duration of the experiment. It has been reported in previous studies that factors such as surface heterogeneity and roughness can cause 'pinning' of the three-phase contact line during dynamic contact angle experiments [52, 55]. For the two solutions with the highest surfactant concentrations, the contact angle exhibits a sudden increase after an initial induction period. The initial steady-state phase for these cases is longer than that of the corresponding surface tension data. This suggests that, while the surface tension is increasing, the contact line remains fixed in place until the rise in surface tension overcomes the 'pinning' and an abrupt increase in contact angle results. For the more dilute solutions, the change in surface tension may be insufficient to liberate the contact line and consequently, no increase in contact angle is observed. Although the contact angle

results presented here are rather limited, it is clear that the surface tension phenomenon does have an influence on certain applications. The results should be improved by investigating a more suitable solid surface for the experiments.

4.6 Summary

In the preceding chapter the experimental investigation on surfactant adsorption and surface tension was presented. The dynamic surface tension profiles for a number of different volatile, organic amphiphiles were measured using the ADSA-P technique. For these compounds it was found that the overall trend in the surface tension is controlled by the concentration difference between the liquid phase and the vapor phase. Initially it seems the surface tension is influenced by the surfactant concentration on both sides of the vapor/liquid interface. However, the final steady-state surface tension seems to be primarily determined by the concentration of surfactant in the vapor phase. Two conventional industrial surfactants were reported as contrast to the results from the organic compounds. Comparing the results from the organic compounds and the conventional surfactants it can be seen that the two exhibit vastly different behavior in terms of surface tension and adsorption.

The surface tension experiments by the ADSA-P method were verified by reproducing select cases using the Wilhelmy plate technique. Although the surface tension values were different in some cases between the two methods, the overall trend in the surface tension was successfully replicated for the 1-octanol and 1-butanol systems. To investigate the behavior of the interface at steady-state conditions, a number of compression and expansion experiments were carried out on the 1-octanol solutions using the ADSA-P method. It was

found that the surface tension responded only when the pendant drop was expanded and the concentration of the drop solution was greater than the concentration of the environment solution.

To illustrate a potential industrial application which may be affected by the observed surface tension phenomenon, time-dependent contact angle experiments were carried out on the 1-octanol solutions. It was observed that, for the more concentrated solutions, the contact angle exhibited an increase over time corresponding to the increase in surface tension of the solution. The results were limited to the solutions with higher surfactant concentrations due to the surface roughness and heterogeneities of the solid substrate chosen for the experiments. It was recommended that a more suitable solid surface be investigated to improve and possibly extend the experimental contact angle results. In the next Chapter the underlying mechanisms involved in the adsorption process will be investigated. Further discussion and corroboration of the experimental observations outlined in the preceding Chapter will also be addressed.

Chapter 5
Theoretical Study of Surfactant Adsorption

5.1 Introduction

In the following chapter the theoretical investigation on surfactant adsorption and surface tension is presented. Due to the unique experimental conditions of this research a number of the empirical and mechanistic models presented here are new or modified forms of current equations and thus, have not been published previously. In Section 5.2 the development of an empirical model examining the relationship between the pendant drop surface tension and the two liquid phase concentrations (drop solution and environment solution) will be discussed. A separate model was considered for both initial and final steady-state conditions. Based on the conclusions from the empirical modeling exercise it was determined that the current mechanistic models would not be applicable to these unique systems. The derivation of a modified equilibrium adsorption isotherm, based on the classic Langmuir analysis, is discussed in Section 5.3. The isotherm was validated with experimental data from a number of the key systems presented in Chapter 4. The modified adsorption isotherm was extended to model the dynamic surface tension behavior of the organic surfactants through the derivation of a new kinetic transfer equation. The development of the transfer equation and the model validation are outlined in Section 5.4. A summary of the theoretical study is given in Section 5.5.

5.2 Empirical Surface Tension Model

In surface science research it is well known that the surface tension of a liquid solution is highly influenced by the liquid phase surfactant concentration. The derivation of nearly every static or dynamic adsorption model is based upon this fact. However, from the results presented in Chapter 4 it is clear that the aqueous surface tension of these organic amphiphiles is affected by the surfactant concentration in the vapor phase, in addition to the liquid phase. Thus, it is desirable to investigate the relationship between the surface tension of these solutions and the surfactant concentration on both sides of the vapor/liquid interface through the development of an empirical model. The dependent variable in the model is the measured surface tension of the pendant drop and the independent variables are the experimental concentrations of the environment solution and the drop solution. The environment solution concentration is used instead of the vapor phase surfactant concentration for simplicity and since the two are directly related through Henry's law.

The compound chosen as the model system for the empirical study was 1-octanol. The experimental data was collected based on a two-factor rotatable central composite design of experiment (CCD). A two-factor CCD augments a base two-factor design with four axial or star points, which facilitates the fitting of a second-order model to the experimental data. The design also provides equal prediction error throughout the region of interest [56]. The concentration layout of the CCD for the empirical study is shown in Figure 5.1. The CCD was designed to span the concentration range of the experimental conditions studied in Chapter 4 and includes four center point replicates to allow for an estimate of the error variance. Each point represents an experimental run corresponding to a specific drop and

environment solution concentration. The proposed CCD was run using the ADSA-P method to generate surface tension data for each point in the design. For each run initial and final steady-state surface tension values were collected and the empirical model was applied at both conditions. The order of the runs was randomized to reduce experimental bias.

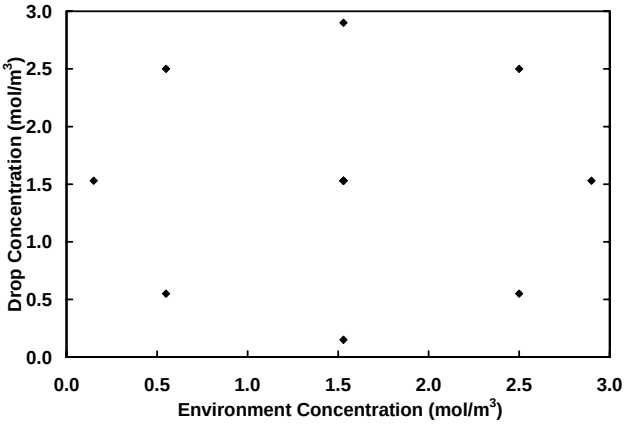

Figure 5.1: Central Composite Design (CCD) of experiment concentration layout for the aqueous 1-octanol empirical surface tension model.

The following model was proposed to predict the surface tension of the liquid solution as a function of concentration:

$$\gamma = \beta_1 + \beta_2 C_{Drop} + \beta_3 C_{Env} + \beta_4 C_{Drop} C_{Env} + \beta_5 C_{Drop}{}^2 + \beta_6 C_{Env}{}^2 \qquad (5.1)$$

where γ is the surface tension of the liquid solution, C_{Drop} is the drop solution concentration, C_{Env} is the environment solution concentration, and $\beta_1 - \beta_6$ are the empirical model coefficients. The model contains linear and quadratic terms for both concentrations as well as an interaction term. The model was truncated at 2nd order since the solution concentration is relatively low and thus, the higher order terms should not have a significant influence on the surface tension. The values of the model coefficients were determined through multiple linear regression with the CCD experimental data. The insignificant terms were removed from the model using a backward elimination method as follows [56]. After regression, the

model coefficients were examined by means of a t-test to determine which, if any, terms were insignificant at the 95% confidence level. The least significant term was removed from the model and the regression was repeated. This process continued until each term remaining in the model was found to be significant.

5.2.1 Initial Steady-State Model

Based on the initial steady-state surface tension data collected from the CCD experimental runs the following empirical model was obtained for the 1-octanol system:

$$\gamma_{initial} = 70.15 - 17.90C_{Drop} - 6.282C_{Env} + 2.033C_{Drop}C_{Env} + 2.411C_{Drop}^{2} \quad (5.2)$$

The quadratic term for the environment solution concentration was found to be statistically insignificant during the regression procedure and was removed from the model. As expected, increasing the drop or environment solution concentration causes a decrease in the initial surface tension. The influence of the drop concentration is greater than the environment concentration based on the magnitude of the coefficients. When the drop and environment solution concentrations are both zero the predicted initial surface tension is 70.15 mN/m which is close to the expected value for pure water (~72 mN/m @ 20°C). The ANOVA statistics for the regression are shown in Table 5.1. Strong agreement between the model predictions and the experimental data is illustrated by the coefficient of determination (R^2) value near 1.0 and the large observed F-statistic shows that the overall regression is significant. The 95% confidence intervals of the model coefficients are shown in

Table 5.2. All parameters were found to be statistically significant at the 95% confidence level due to the fact that none of the intervals span zero. Due to the statistical significance of the empirical model it can be concluded that Equation (5.2) can provide accurate estimates of

the initial surface tension of aqueous 1-octanol solutions across the experimental concentration range studied.

Table 5.1: ANOVA table for the 1-octanol initial steady-state empirical surface tension model.

Source	Degrees of Freedom	Sum of Squares	Mean Square	F-Statistic	R^2
Regression	4	2013.71	503.43	218.15	0.9842
Residual	14	32.31	2.308		
Total	18	2046.01			

Table 5.2: 95% confidence intervals for the empirical parameters in the 1-octanol initial steady-state surface tension model.

95% Confidence Intervals		
68.18	$< \beta_1 <$	72.12
-21.14	$< \beta_2 <$	-14.67
-7.793	$< \beta_3 <$	-4.770
1.085	$< \beta_4 <$	2.980
1.392	$< \beta_5 <$	3.430

The validity of the empirical model was assessed by using the model to predict the initial steady-state surface tension of existing experimental data where the drop and environment solution concentrations were known. A comparison of the model predictions and the measured experimental data is shown in Figure 5.2A. The model exhibits strong predictive power based on the excellent agreement between the model predictions and the experimental data. There are some deviations at very high or very low values of initial surface tension possibly due to the large experimental range of the CCD. A three-dimensional surface response plot of the model predictions over the entire experimental concentration range is shown in Figure 5.2B.

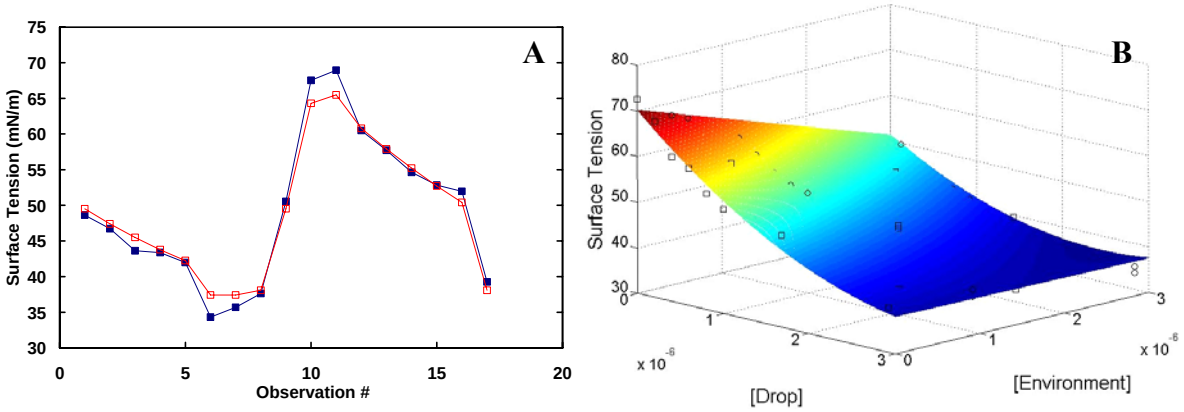

Figure 5.2: Model predictions for the 1-octanol initial steady-state empirical surface tension model. (A) Comparison of model predictions (□) with existing experimental data (■). (B) Three-dimensional surface response plot of model predictions over the entire experimental concentration range along with existing experimental data (□, ○).

5.2.2 Final Steady-State Model

Based on the final steady-state surface tension data collected from the CCD experimental runs the following empirical model was obtained for the 1-octanol system:

$$\gamma_{final} = 69.74 - 20.86C_{Env} + 3.264C_{Env}^{\ 2} \qquad (5.3)$$

All terms involving the drop solution concentration were found to be statistically insignificant during the regression and thus, were removed from the model. The model implies that the final steady-state surface tension is a quadratic function of the environment solution concentration and is independent of the drop solution concentration. The statistical results support the observation from the experimental study (Chapter 4) that the surface tension at final steady-state conditions is primarily determined by the surfactant concentration in the vapor phase. The ANOVA statistics for the regression are shown in Table 5.3. Strong agreement between the model predictions and the experimental data is illustrated by the coefficient of determination (R^2) value near 1.0 and the large observed F-statistic shows that the overall regression is significant. The 95% confidence intervals of the model coefficients are shown in Table 5.4. All parameters were found to be statistically

significant at the 95% confidence level due to the fact that none of the intervals span zero. The statistical significance of the empirical model illustrates that Equation (5.3) can provide accurate estimates of the final steady-state surface tension of aqueous 1-octanol solutions across the experimental concentration range studied.

Table 5.3: ANOVA table for the 1-octanol final steady-state empirical surface tension model.

Source	Degrees of Freedom	Sum of Squares	Mean Square	F-Statistic	R^2
Regression	2	1420.58	710.29	274.56	0.9821
Residual	10	25.87	2.587		
Total	12	1446.45			

Table 5.4: 95% confidence intervals for the empirical parameters in the 1-octanol final steady-state surface tension model.

95% Confidence Intervals		
67.30	$< \beta_1 <$	72.18
-24.58	$< \beta_2 <$	-17.13
1.999	$< \beta_3 <$	4.529

The validity of the empirical model was assessed by using the model to predict the final steady-state surface tension of existing experimental data where the drop and environment solution concentrations were known. A comparison of the model predictions and the measured experimental data is shown in Figure 5.3A. The model exhibits strong predictive power based on the excellent agreement between the model predictions and the experimental data. The model predictions over the entire experimental concentration range are shown in Figure 5.3B. Again excellent agreement between the model predictions and experimental data is observed.

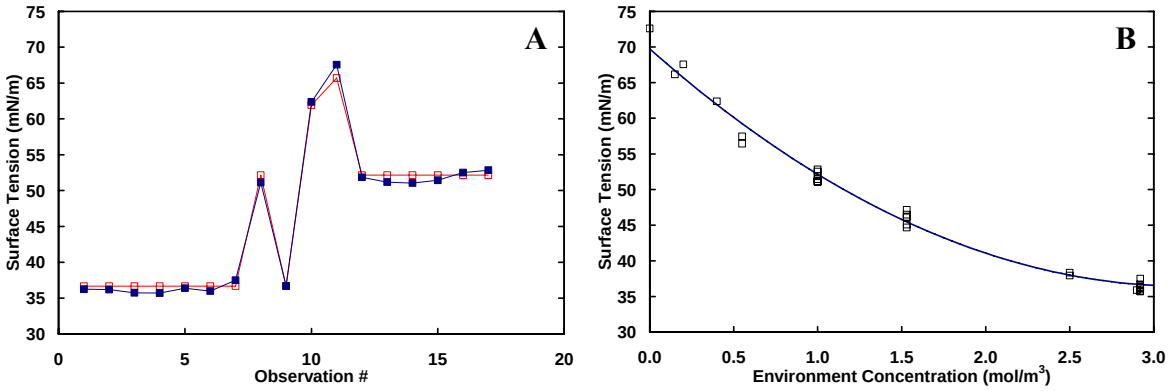

Figure 5.3: Model predictions for the 1-octanol final steady-state empirical surface tension model. (A) Comparison of model predictions (□) with existing experimental data (■). (B) Model predictions over the entire experimental concentration range along with existing experimental data (□).

5.3 Modified Adsorption Isotherm

The purpose of an equilibrium adsorption isotherm is to relate the surfactant concentration in the bulk and the amount adsorbed at the interface [28]. Given the proper adsorption isotherm along with the Gibbs adsorption equation, one can derive a corresponding surface equation of state that gives the equilibrium surface tension as a function of surfactant concentration. The most commonly used adsorption isotherms include the Henry isotherm, the Langmuir isotherm, and the Frumkin isotherm [28, 29], as well as various modifications of those mentioned [19, 25]. These isotherms account for surfactant adsorption from the bulk liquid phase to the interface. From the results of the experimental study presented in Chapter 4 and the empirical modeling exercise outlined in the Section 5.2, it is clear that for these systems adsorption from the liquid and the vapor phase contributes to the surfactant concentration at the interface. Thus, for the theoretical analysis a new or modified adsorption isotherm is required to accurately model the adsorption behavior of the organic amphiphiles investigated in this research. The derivation and validation of the modified adsorption isotherm is outlined in the following section.

5.3.1 Adsorption Isotherm Derivation

In the derivation of the classic Langmuir isotherm, adsorption from either the liquid phase or the vapor phase, to the interface, was considered. As a result the Langmuir adsorption isotherm is a relation between the interfacial surfactant concentration and either the concentration in the bulk liquid phase or the partial pressure of the vapor phase [13]. However, in the current systems adsorption from the liquid and the vapor phase contribute to the surface concentration simultaneously. Thus, the modified adsorption isotherm must account for dual adsorption from both sides of the vapor/liquid interface. The derivation will follow the same rational and level of assumptions as the classic Langmuir isotherm due to its broad range of applicability. The first step in the derivation is to write expressions for the rates of adsorption and desorption to and from either side of the vapor/liquid interface:

$$r_a^g = k_a^g P S_o = k_a^g P(S - S_1) \tag{5.4}$$

$$r_d^g = k_d^g S_1 \tag{5.5}$$

$$r_a^l = k_a^l C S_o = k_a^l C(S - S_1) \tag{5.6}$$

$$r_d^l = k_d^l S_1 \tag{5.7}$$

where r_a^g, r_d^g, r_a^l, r_d^l are the rates of adsorption and desorption in the vapor and liquid phase, respectively, k_a^g, k_d^g, k_a^l, k_d^l, are the kinetic rate constants for adsorption and desorption in the vapor and liquid phase, respectively, P is the partial pressure of surfactant in the vapor phase, C is the concentration of surfactant in the liquid phase, S is the total number of adsorption sites at the interface, S_o is the number of free adsorption sites, and S_1 is the number of occupied adsorption sites. The model follows Langmuir kinetics where the rates of adsorption are proportional to the surfactant concentration and the number of vacant adsorption sites at the interface ($S - S_1$), and the rate of desorption is proportional to the

surface coverage (S_1) [28]. At steady-state or equilibrium, the overall rate of adsorption is equal to the overall rate of desorption. Equating the expressions for the rates of adsorption and desorption leads to:

$$k_a^g P(S - S_1) + k_a^l C(S - S_1) = k_d^g S_1 + k_d^l S_1 \tag{5.8}$$

Equation (5.8) can be simplified to obtain the modified Langmuir adsorption isotherm:

$$S_1 / S = \Gamma / \Gamma_\infty = \frac{K_1 P + K_2 C}{1 + K_1 P + K_2 C} \tag{5.9}$$

$$K_1 = \frac{k_a^g}{k_d^g + k_d^l} \tag{5.10}$$

$$K_2 = \frac{k_a^l}{k_d^g + k_d^l} \tag{5.11}$$

where Γ is the surface concentration of surfactant, Γ_∞ is the maximum surface concentration, and K_1 and K_2 are the equilibrium constants for adsorption from the vapor phase and the liquid phase, respectively. Equation (5.9) describes the steady-state relationship between the concentration of surfactant at the interface and its partial pressure in the vapor phase and concentration in the liquid phase. In order to relate the surface concentration of surfactant to surface tension, an appropriate surface equation of state must be utilized. From the Gibb's adsorption equation [Equation (2.2)] the following equation of state can be derived which is consistent with Langmuir-type kinetics and has been used extensively in the literature [57]:

$$\gamma = \gamma_o + \Gamma_\infty RT \ln\left(1 - \Gamma / \Gamma_\infty\right) \tag{5.12}$$

where γ is the surface tension of the solution, γ_o is the surface tension of the pure solvent, R is the universal gas constant, and T is the temperature. The final form of the surface equation of state can be obtained by combining Equations (5.9) and (5.12) and relating the partial

pressure of surfactant in the vapor phase (P) to the concentration of the environment solution (C_{env}) through Henry's law $\left(P = H\,C_{env}\right)$ [58]:

$$\gamma = \gamma_o - \Gamma_\infty RT \ln\left(1 + K_1 H C_{env} + K_2 C_{drop}\right) \tag{5.13}$$

where H is the Henry's law constant for the surfactant in aqueous solution, C_{env} is the concentration of surfactant in the environment solution, and C_{drop} is the concentration of surfactant in the drop solution. The modified Langmuir adsorption isotherm [Equation (5.9)] and corresponding surface equation of state [Equation (5.13)] are the first of their kind for predicting the steady-state surface tension of a liquid solution as a function of surfactant concentration in the liquid phase and the vapor phase. The equilibrium parameters K_1, K_2, and Γ_∞, can be determined for any system by fitting Equation (5.13) to experimental data through nonlinear regression. In the next section the validation of the modified adsorption isotherm will be discussed.

5.3.2 Adsorption Isotherm Validation

The modified Langmuir adsorption isotherm and corresponding surface equation of state were validated by applying the equations to three of the key systems studied in Chapter 4. The equilibrium parameters K_1, K_2, and Γ_∞, were determined for 1-butanol, 1-hexanol, and 1-octanol by fitting Equation (5.13) to experimental data through nonlinear regression. The parameters were generated at both initial and final steady-state conditions using data from the central composite design (CCD) of experiment for 1-octanol, and existing experimental data for 1-butanol and 1-hexanol. The optimization routine was implemented in MATLAB and the parameters were obtained by minimizing the residual sum of squares between the model predictions and the experimental data. It is expected that the parameter values between the initial and final steady-state fittings should illustrate a similar trend as the empirical model in

terms of which phase (liquid or vapor) has a significant influence on the measured surface tension. The least squares estimates of the equilibrium parameters for the three systems are shown in Table 5.5. The model predictions from the surface equation of state corresponding to the parameter values in Table 5.5 are shown in Figure 5.4 for 1-butanol, Figure 5.5 for 1-hexanol, and Figure 5.6 for 1-octanol. In all cases the model predictions exhibit strong agreement with the experimental data.

Table 5.5: Equilibrium parameters for the modified Langmuir adsorption isotherm.

Surfactant	Fitting	Γ_∞ (mol/m^2)	K_1[a] (m^3/mol)	K_2 (m^3/mol)
Butanol	Initial	5.91×10^{-6}	0.0063	0.0205
	Equilibrium	5.95×10^{-6}	0.0216	0.0007
Hexanol	Initial	6.86×10^{-6}	0.0320	0.2033
	Equilibrium	6.31×10^{-6}	0.2169	0.0052
Octanol	Initial	8.19×10^{-6}	0.6440	1.4316
	Equilibrium	7.87×10^{-6}	1.9188	0.0887

[a] The values of K_1 include the Henry's law constant so that the units are uniform with K_2

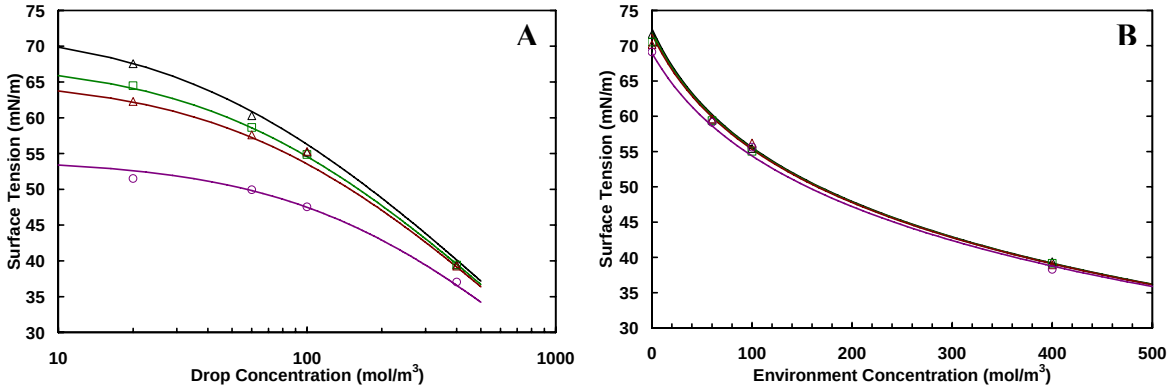

Figure 5.4: (A) Initial steady-state surface tension of aqueous 1-butanol as a function of drop solution concentration for C_{env} = 0 mol/m^3 (Δ), 60 mol/m^3 (□), 100 mol/m^3 (Δ), and 400 mol/m^3 (○). (B) Final steady-state surface tension of aqueous 1-butanol as a function of environment solution concentration for C_{drop} = 20 mol/m^3 (Δ), 60 mol/m^3 (□), 100 mol/m^3 (Δ), and 400 mol/m^3 (○). Solid lines represent theoretical predictions from Equation (5.13) corresponding to the parameter values in Table 5.5.

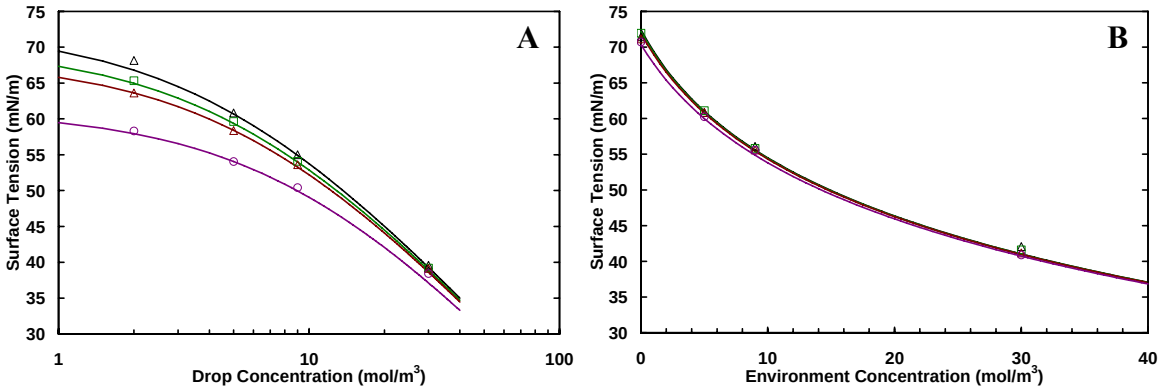

Figure 5.5: (A) Initial steady-state surface tension of aqueous 1-hexanol as a function of drop solution concentration for C_{env} = 0 mol/m^3 (Δ), 5 mol/m^3 (□), 9 mol/m^3 (Δ), and 30 mol/m^3 (○). (B) Final steady-state surface tension of aqueous 1-hexanol as a function of environment solution concentration for C_{drop} = 2 mol/m^3 (Δ), 5 mol/m^3 (□), 9 mol/m^3 (Δ), and 30 mol/m^3 (○). Solid lines represent theoretical predictions from Equation (5.13) corresponding to the parameter values in Table 5.5.

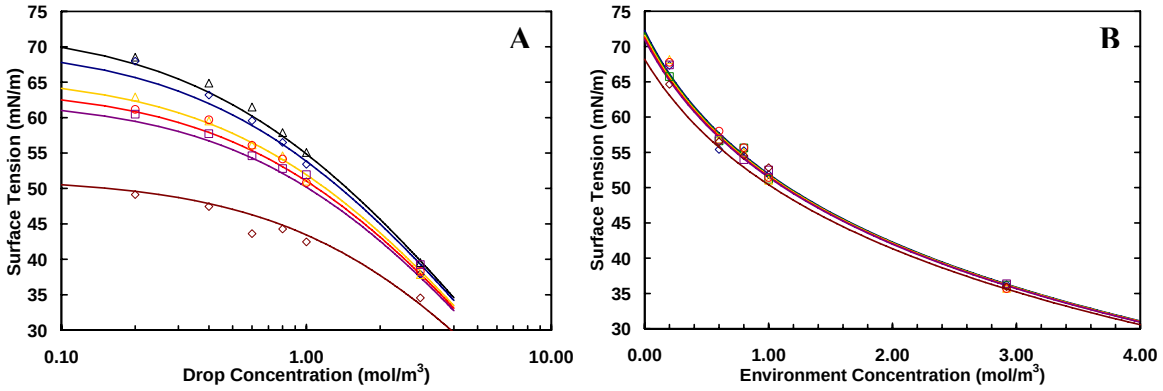

Figure 5.6: (A) Initial steady-state surface tension of aqueous 1-octanol as a function of drop solution concentration for C_{env} = 0 mol/m^3 (Δ), 0.2 mol/m^3 (◊), 0.6 mol/m^3 (Δ), 0.8 mol/m^3 (○), 1.0 mol/m^3 (□), and 2.92 mol/m^3 (◊). (B) Final steady-state surface tension of aqueous 1-octanol as a function of environment solution concentration for C_{drop} = 0.2 mol/m^3 (◊), 0.4 mol/m^3 (□), 0.6 mol/m^3 (Δ), 0.8 mol/m^3 (○), 1.0 mol/m^3 (□), and 2.92 mol/m^3 (◊). Solid lines on both graphs represent theoretical predictions from Equation (5.13) corresponding to the parameter values in Table 5.5.

Examining the equilibrium parameter values in Table 5.5 it can be seen that for all three surfactants the maximum surface concentration (Γ_∞) is very similar for the initial and final steady-state fittings and compare well with published values [18, 19, 25, 29]. This is expected as the parameter is a function of the physical size of a given molecule at the surface

and thus, should be constant. In general, Γ_∞ increases slightly with increasing carbon chain length. This is most likely due to increased surface area coverage of the longer molecules caused by imperfect arrangement at the surface. Looking at the adsorption equilibrium constants it can be seen that K_1 and K_2 differ considerably between the initial and final fittings for a given surfactant. Also, the value of K_1 is often quite different than the value of K_2 in any given case. As previously stated, the adsorption equilibrium constants are often used as a gauge of the surface activity or efficiency of a surfactant [29]. A large value implies the surfactant is more surface active or conducive to adsorption and thus, more efficient at reducing the surface tension in solution. Therefore, the value of K_1 is indicative of the contribution to adsorption from the vapor phase and the value of K_2 is indicative of the contribution from the liquid phase. For a given surfactant the difference in the values of K_1 and K_2 between the two fittings illustrates the difference in adsorption at initial and final steady-state conditions.

Examining the adsorption equilibrium constants in Table 5.5 for any given surfactant one can see that initially both the liquid and the vapor phase contribute to adsorption at the interface as illustrated by the comparable values of K_1 and K_2. At final steady-state conditions, adsorption from the vapor phase represents the major contribution as reflected by the difference in the magnitudes of K_1 and K_2 (K_2 is only 3.2% of K_1 for 1-butanol, 4.6% for 1-octanol, and 2.4% for 1-hexanol). In general, the values of the adsorption constants increase from 1-butanol to 1-octanol indicating an increase in surface activity with hydrocarbon chain length. The phenomenon of increasing tensioactivity with chain length is described by Traube's rule, and has been observed in previous studies [29, 38]. The results support the

experimental observations discussed in Chapter 4, as well as the conclusions based on the empirical model that initially the surface tension is determined by a combination of adsorption from the liquid and the vapor phase, whereas at the final steady-state the surface tension is determined primarily by adsorption from the surrounding vapor.

At the final steady-state conditions or experimental "equilibrium", molecular exchange between the liquid phase and the interface becomes severely diminished, implying that a significant energy barrier may have been forged on the liquid side of the interface. Previous molecular dynamics simulations have shown that the headgroups of alcohol molecules tend to cluster together in aqueous solution and form highly structured, hydrogen bonded networks with surrounding water molecules [59, 60]. The presence of this surfactant network near the interface may play a role in the loss of molecular exchange between the liquid phase and the interface at the final steady-state. To explore this hypothesis the dynamic surface tension of a 1-octanol solution was measured for consecutive drops from a continuous run using the same syringe and environment solution. In this experiment, the surface tension of the first drop was measured according to the normal procedure. At the end of the run, the drop was discharged into the environment and a second drop was formed without removing the syringe from the chamber. The surface tension of the second drop was then measured until it was no longer changing. The results from the experiment are shown in Figure 5.7. The profiles from the two consecutive runs are nearly identical proving that, even at the final steady-state conditions, the concentration difference between the liquid phase and the vapor phase is maintained. This implies that, at steady-state conditions, a true thermodynamic equilibrium has not been reached.

These results, along with the expansion experiments (Figure 4.11), provide support for the theory of a surfactant network or energy barrier to molecular transport between the bulk liquid and the interface. At steady-state conditions the drop solution behaves as though its concentration is equal to the concentration of the environment solution. However, the expansion and consecutive drop experiments suggest that concentration of the drop solution is maintained. Logically one may suspect that at steady-state conditions the concentration of the two liquid phases (drop and environment) should be equal. If this were true the steady-state concentration should lie somewhere between the initial concentrations of the drop and environment solutions, and the surface tension should reflect this intermediate concentration. In reality the steady-state surface tension of the pendant drop is characteristic of the environment solution, implying that the concentration of the drop solution is the same as the concentration of the environment solution. This, however, is not possible based on fundamental thermodynamic arguments. For these reasons it is speculated that at steady-state conditions the behavior of the drop solution is dominated by the vapor phase. Molecular transport between the bulk liquid and the interface becomes diminished due to the presence of a hydrogen bonded surfactant network in the liquid phase. The interface behaves as though the concentration of the drop solution is equal to the concentration of the environment solution even though the concentration difference between the two phases is maintained.

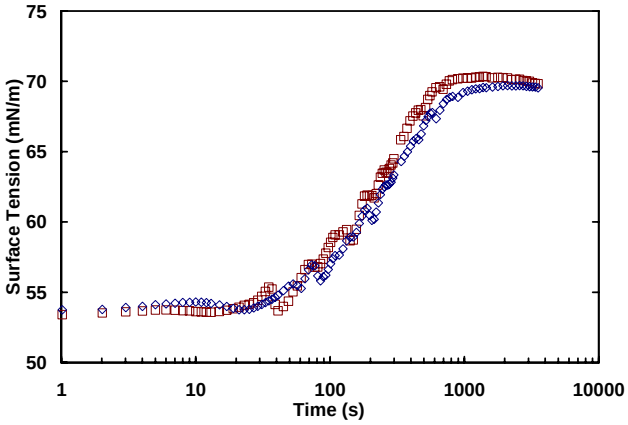

Figure 5.7: Aqueous 1-octanol dynamic surface tension profiles for consecutive drops from a continuous run using the same syringe and environment solution; Drop #1 (□), Drop #2 (◊). Drop solution concentration is 1.0 mol/m^3 and environment solution is pure water.

5.4 Dynamic Surface Tension Model

In the previous section the equilibrium, or steady-state, relation between surface tension and adsorption was investigated theoretically through the derivation of a new adsorption isotherm based on similar rationale and approximations of the Langmuir isotherm. The modified isotherm was designed to account for adsorption from both sides of the vapor/liquid interface simultaneously and was shown to accurately model the steady-state surface tension data of the systems studied. In this section, the equilibrium isotherm is extended to model the dynamics of adsorption through the creation of a new kinetic transfer equation. As with the steady-state analysis the transfer equation must simulate simultaneous adsorption/desorption from both sides of the interface in order to accurately model the system dynamics.

As discussed previously, the dynamic adsorption behavior of surfactant solutions is governed by a two-step process involving diffusion of molecules from the bulk solution to the subsurface and kinetic transfer between the subsurface and the interface [29]. The adsorption kinetics are typically characterized based on the rate-limiting step of this process and most

theoretical models have been developed for either diffusion-controlled or mixed diffusion/transfer-controlled mechanisms [28]. However, if the rate of diffusion is much faster than the transfer step, the adsorption is considered to be transfer-controlled and the entire process can be described by a kinetic model [61]. Previous studies have reported that the adsorption kinetics of normal alcohols with short carbon chains are controlled primarily by transfer of surfactant from the subsurface to the interface [18, 38]. Thus, for simplicity, the new kinetic transfer equation developed here was validated against dynamic surface tension data from the two surfactants studied with the shortest carbon chain lengths (1-butanol and 1-hexanol). Using data from transfer-controlled systems avoids the need to solve the diffusion and transfer equations simultaneously and provides a clear assessment of the applicability of the new transfer equation. Thus, the legitimacy of the transfer equation was assessed based on the ability to accurately model the data from these two systems.

5.4.1 Kinetic Transfer Equation Derivation

The equilibrium adsorption isotherm gives the surface concentration of surfactant at steady-state conditions. The kinetic transfer equation describes the change in surface concentration with time during non-equilibrium conditions. Due to the relation between the two, the transfer equation should be consistent with the equilibrium adsorption isotherm for a given system. This means that at steady-state conditions $\left(d\Gamma/dt = 0\right)$, the transfer equation should reduce to the equilibrium adsorption isotherm. Similar to the derivation of the adsorption isotherm, both sides of the vapor/liquid interface must be considered simultaneously due to the unique experimental conditions of this research. Therefore, the transfer equation will contain adsorption and desorption terms corresponding to the liquid side and the vapor side of the interface.

At steady-state, the overall rate of adsorption is equal to the overall rate of desorption [Equation (5.8)]. For unsteady-state the change in surface concentration over time can be expressed as the net rate of adsorption minus the net rate of desorption:

$$d\Gamma/dt = \left(r_a^g + r_a^l\right) - \left(r_d^g + r_d^l\right) \tag{5.14}$$

where r_a^g, r_d^g, r_a^l, and r_d^l are defined by Equations (5.4) – (5.7). Similar to the adsorption isotherm, the transfer equation follows Langmuir kinetics where the rates of adsorption are proportional to the surfactant concentration and the number of vacant adsorption sites at the interface ($\Gamma_\infty - \Gamma$), and the rate of desorption is proportional to the surface coverage (Γ) [28]. Substituting in the appropriate expressions for the rates of adsorption and desorption gives:

$$d\Gamma/dt = k_a^g C_{env}(\Gamma_\infty - \Gamma) + k_a^l C_{drop}(\Gamma_\infty - \Gamma) - (k_d^g + k_d^l)\Gamma \tag{5.15}$$

where k_a^g and k_a^l are the adsorption rate constants for the vapor and the liquid phase, respectively, and k_d^g and k_d^l are the desorption rate constants for the vapor and the liquid phase, respectively. For the vapor phase adsorption rate, the partial pressure of surfactant (P) was related to the concentration of the environment solution (C_{env}) through Henry's Law $\left(P = H\,C_{env}\right)$ [58], as in the derivation of the adsorption isotherm. It should be noted that the Henry's law constant has been incorporated into k_a^g so the units of the adsorption rate constants are uniform. For solution purposes it is desirable to reduce the number of unknown constants in Equation (5.15) using the adsorption equilibrium constants (K_1 and K_2) which were determined during the steady-state analysis. From their definitions the following simplifications can be made:

$$k_d^g + k_d^l = \frac{k_a^g + k_a^l}{K_1 + K_2} \tag{5.16}$$

$$k_a^l = k_a^g \, K_2 \Big/ K_1 \tag{5.17}$$

Substitution into Equation (5.15) eliminates all but one of the kinetic rate constants:

$$d\Gamma \Big/ dt = k_a^g \left(C_{env} + K_2 \Big/ K_1 \, C_{drop} \right)(\Gamma_\infty - \Gamma) - \frac{k_a^g}{K_1 + K_2} \left(1 + K_2 \Big/ K_1 \right)\Gamma \tag{5.18}$$

Equation (5.18) is separable and can be integrated directly to give the surface concentration of surfactant as a function of time Γ(t). Since the surface concentration is not a measurable quantity with time, a relation between γ(t) and Γ(t) is required. A generally accepted assumption is that the relationship between the surface tension and surface concentration is the same as at equilibrium [29]. In our case this relation is the Frumkin equation, which is consistent with the Langmuir approximation and was also applied in the derivation of the adsorption isotherm:

$$\gamma = \gamma_o + \Gamma_\infty RT \ln\left(1 - \Gamma \Big/ \Gamma_\infty \right) \tag{5.19}$$

Thus, Equation (5.18) can be solved in conjunction with Equation (5.19) to yield a theoretical prediction of γ(t). The vapor phase adsorption rate constant (k_a^g) can be evaluated through nonlinear regression with experimental dynamic surface tension data. The liquid phase constant (k_a^l) can then be calculated from Equation (5.17) and the theoretical predictions of γ(t) can be compared with the experimental data to assess the validity of the model.

The values of K_1 and K_2 used during the model solution will be taken from the initial surface tension fitting. Typically for this type of simplification, the equilibrium constants are obtained at final steady-state conditions. However, since most studies involving these types of surfactants investigate short adsorption times (millisecond to second range), the

equilibrium conditions of those studies would correspond to the initial conditions of the current research. Furthermore, the constants at initial conditions better reflect the influence of both the liquid phase and the vapor phase on the adsorption dynamics since, at that time, both are significant.

5.4.2 Kinetic Transfer Equation Validation

The kinetic transfer equation was validated against dynamic surface tension data from two of the systems studied in Chapter 4. The transfer equation was fit to the experimental data through a nonlinear regression routine where the vapor phase adsorption rate constant (k_a^g) is treated as a fitting parameter. The optimization routine was implemented in MATLAB and the value of k_a^g was obtained by minimizing the residual sum of squares between the model predictions and the experimental data. Thus, a distinct value for k_a^g was obtained for each dynamic surface tension profile, and was used to calculate the liquid phase adsorption rate constant (k_a^l). It is expected that the values of k_a^g and k_a^l should not change significantly for a given surfactant.

The theoretical predictions from the modified Langmuir kinetic transfer equation are plotted along with the experimental data in Figure 5.8 for 1-butanol and Figure 5.9 for 1-hexanol. In most cases, the modified transfer equation fits the experimental data quite well. The only notable discrepancies occur when the concentration difference between the liquid phase and the vapor phase is the largest. Interestingly, the deviations are present at the same conditions for both 1-butanol and 1-hexanol. Previous studies have reported that alcohol molecules exhibit a cooperative effect for adsorption at high surfactant concentrations due to intermolecular attraction at the interface [19, 23, 25]. The cohesive forces among the

adsorbed molecules raise the energy barrier for desorption into the bulk and thus, lower the rate of desorption. It is possible that for these cases the interactions between surfactant molecules at the interface become significant because of the high surfactant concentration causing the error in the theoretical predictions. It should be noted that the zero concentration difference cases ($C_{drop} = C_{env}$) were omitted from the analysis since the transfer equation does not apply at these conditions. When the drop solution concentration is equal to the environment solution concentration there is no driving force for surfactant transfer and the surface tension remains essentially constant (i.e. $d\Gamma/dt = 0$).

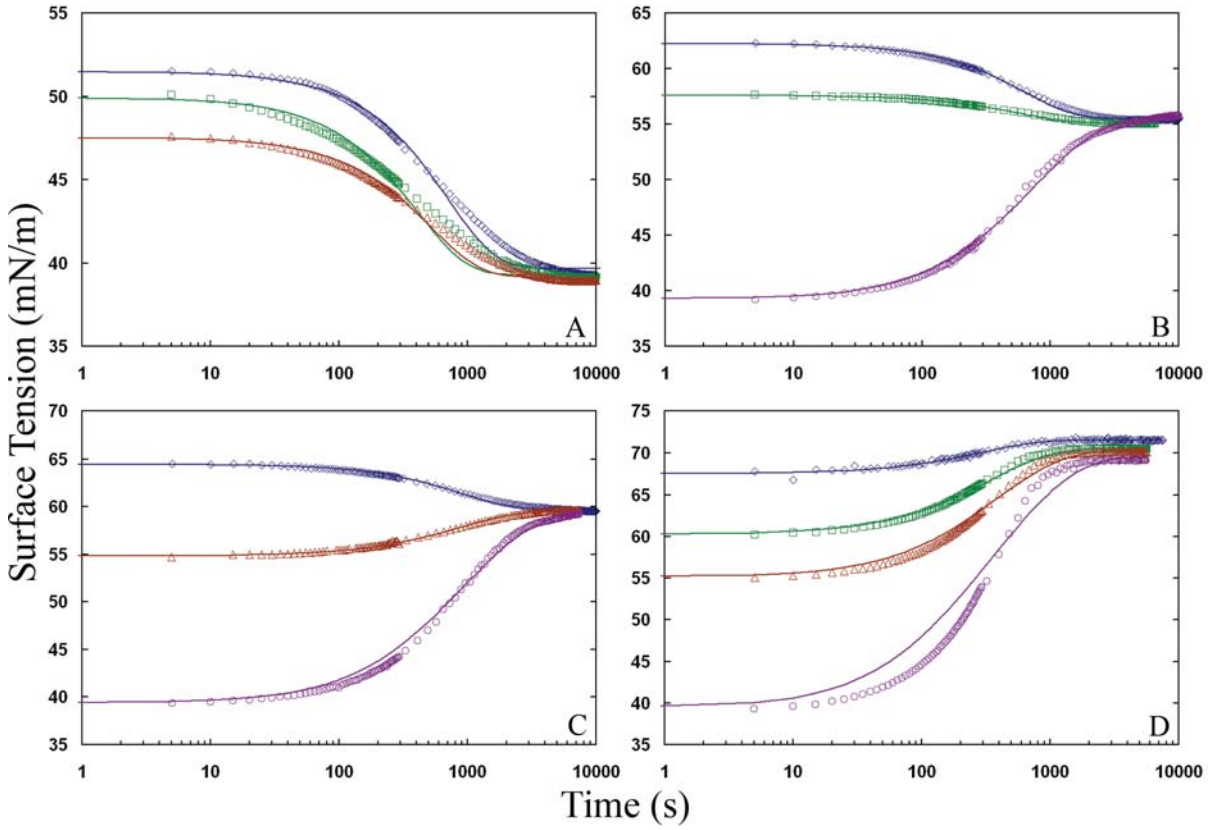

Figure 5.8: Kinetic transfer equation theoretical predictions (solid lines) for aqueous 1-butanol solutions with C_{drop} = 20 mol/m^3 (◊), 60 mol/m^3 (□), 100 mol/m^3 (Δ), and 400 mol/m^3 (○). Each graph represents a different environment solution concentration (C_{env}); (A) 400 mol/m^3, (B) 100 mol/m^3, (C) 60 mol/m^3, and (D) pure water.

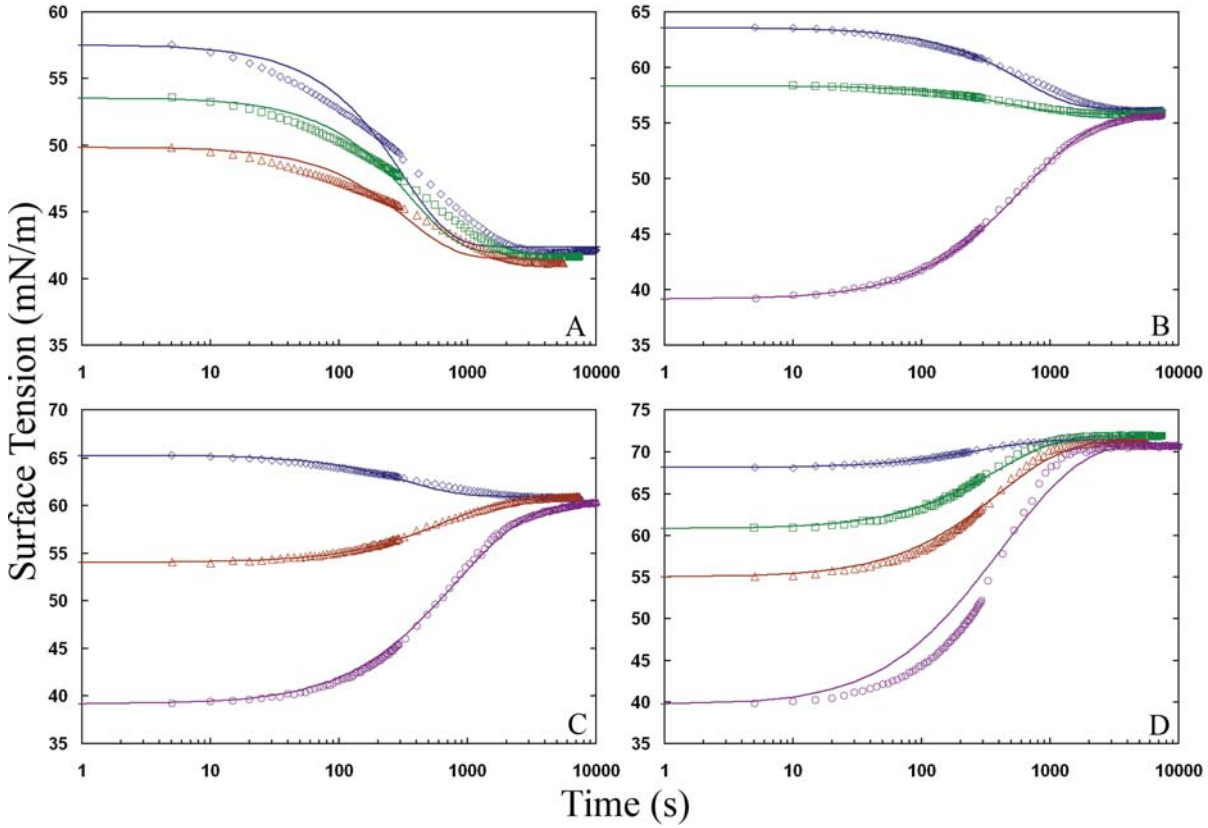

Figure 5.9: Kinetic transfer equation theoretical predictions (solid lines) for aqueous 1-hexanol solutions with C_{drop} = 2 mol/m^3 (◊), 5 mol/m^3 (□), 9 mol/m^3 (Δ), and 30 mol/m^3 (○). Each graph represents a different environment solution concentration (C_{env}); (A) 30 mol/m^3, (B) 9 mol/m^3, (C) 5 mol/m^3, and (D) pure water.

The kinetic rate constants corresponding to the theoretical predictions in Figure 5.8 and Figure 5.9 are shown in Table 5.6. Although theoretically these values should be constant regardless of the surfactant concentration, several studies have reported rate constants that vary to some degree with concentration even though the two may not necessarily be correlated [19, 23, 25, 29, 62]. Other factors that have been reported to influence the magnitude of the kinetic rate constants include the degree of saturation of the adsorption layer and its lifetime.

The average values for k_a^g are $4.08x10^{-6} \pm 2.73x10^{-6}$ $m^3/mol•s$ with a variance of $7.45x10^{-12}$ $m^3/mol•s$ for 1-butanol and $3.23x10^{-5} \pm 1.98x10^{-5}$ $m^3/mol•s$ with a variance of $3.92x10^{-10}$ $m^3/mol•s$ for 1-hexanol. For k_a^l the average values are $1.33x10^{-5} \pm 8.91x10^{-6}$ $m^3/mol•s$ with a variance of $7.94x10^{-11}$ $m^3/mol•s$ for 1-butanol and $2.05x10^{-4} \pm 1.26x10^{-4}$ $m^3/mol•s$ with a variance of $1.58x10^{-8}$ $m^3/mol•s$ for 1-hexanol. The spread of the constants, as measured by the standard deviation, is less than one order of magnitude and the variance is at least double the order of magnitude lower than the value of the constants in all cases. For both systems the values of k_a^l are generally larger than k_a^g, and the magnitudes of the rate constants increase from 1-butanol to 1-hexanol, which reflects the increase in surface activity with carbon chain length.

Table 5.6: Adsorption rate constants for the modified Langmuir kinetic transfer equation.

Surfactant	Temperature (°C)	Environment Concentration (mol/m^3)	Drop Concentration (mol/m^3)	k_a^g ($m^3/mol\ s$)	k_a^l ($m^3/mol\ s$)
Butanol	25	400	100	$2.21x10^{-6}$	$7.20x10^{-6}$
			60	$3.39x10^{-6}$	$1.11x10^{-5}$
			20	$2.45x10^{-6}$	$7.98x10^{-6}$
		100	100	$1.09x10^{-6}$	$3.56x10^{-6}$
			60	$3.96x10^{-6}$	$1.29x10^{-5}$
			20	$5.79x10^{-6}$	$1.89x10^{-5}$
		60	400	$9.56x10^{-7}$	$3.12x10^{-6}$
			100	$2.13x10^{-6}$	$6.96x10^{-6}$
			20	$4.62x10^{-6}$	$1.51x10^{-5}$
		Pure Water	400	$3.27x10^{-6}$	$1.07x10^{-5}$
			100	$5.18x10^{-6}$	$1.69x10^{-5}$
			60	$7.12x10^{-6}$	$2.32x10^{-5}$
			20	$1.09x10^{-5}$	$3.55x10^{-5}$
Hexanol	25	30	9	$2.60x10^{-5}$	$1.65x10^{-4}$
			5	$3.29x10^{-5}$	$2.09x10^{-4}$
			2	$5.42x10^{-5}$	$3.44x10^{-4}$
		9	30	$7.85x10^{-6}$	$4.98x10^{-5}$
			5	$3.04x10^{-5}$	$1.93x10^{-4}$
			2	$4.03x10^{-5}$	$2.56x10^{-4}$
		5	30	$6.59x10^{-6}$	$4.18x10^{-5}$
			9	$1.52x10^{-5}$	$9.64x10^{-5}$
			2	$7.15x10^{-5}$	$4.54x10^{-4}$
		Pure Water	30	$1.64x10^{-5}$	$1.04x10^{-4}$
			9	$2.66x10^{-5}$	$1.69x10^{-4}$
			5	$3.30x10^{-5}$	$2.09x10^{-4}$
			2	$5.94x10^{-5}$	$3.77x10^{-4}$

The obvious limitation of this type of model is the variation in the kinetic rate constants. This is a limitation of any adsorption model that employs fitting parameters to optimize the model predictions and is present in many other kinetic adsorption studies. There are many factors, such as the presence of impurities, temperature fluctuations, and loss of surfactant due to vapor leakage that may skew the experimental data away from the theoretical. The transfer equation is essentially an empirical model and, although it is based on sound theory, any imperfections in the experimental data will inevitably be reflected in the values obtained for the kinetic rate constants. Furthermore, the experimental data represents a wide range of surfactant concentrations (drop solution and environment solution), which is bound to magnify the variation. Having said that, it may be possible to identify certain regions in the data where the variation is most pronounced and thus, where the model is less valid. Examining the data in Table 5.6 we can see that deviations that exceed one standard deviation from the mean seem to occur when the concentration (drop-environment) is either low-low or high-moderate. The trend is present across both systems. This indicates that the model may be best suited for concentrations where these particular combinations are avoided.

Regardless of the outlined limitations, the experimental data is represented well by the model predictions. If the conditions discussed above are avoided, the model succeeds in predicting the experimental data and generating suitable kinetic rate constants. The results support the validity of the modified Langmuir kinetic transfer equation and illustrate the importance of the vapor phase in describing the adsorption kinetics of this class of organic molecules. The

transfer equation can be used to model the adsorption dynamics of systems where the surface tension is influenced by surfactant adsorption and desorption from both sides of the vapor/liquid interface. Furthermore, the results prove that the dynamic surface tension for the adsorption of normal alcohols with short carbon chains can be described by a transfer controlled kinetic mechanism.

5.5 Summary

In this chapter the theoretical study of surfactant adsorption and surface tension was presented. An empirical model was developed which described the relationship between the steady-state surface tension and the surfactant concentration of the drop and environment solutions at initial and final conditions. It was found that initially both concentrations were significant in predicting the surface tension, while the final steady-state surface tension was determined to be a quadratic function of the environment solution concentration and independent of the drop solution concentration. The statistical results are consistent with the observations made based on the experimental study discussed in Chapter 4.

Based on the empirical analysis it was determined that in order to accurately describe the steady-state conditions of these systems a modified adsorption isotherm, which incorporates adsorption from both sides of the vapor/liquid interface, would be required. The derivation was based on the same rational and level of assumptions as the classic Langmuir isotherm while considering vapor and liquid phase adsorption simultaneously. The modified isotherm was combined with the Gibbs adsorption equation to create a new surface equation of state which was used to generate the equilibrium parameters (Γ_∞, K_1, and K_2) for 1-butanol, 1-

hexanol, and 1-octanol through nonlinear regression with experimental data. The values obtained for the maximum surface concentration (Γ_∞) agreed well with literature values for these components. The values of the equilibrium adsorption constants (K_1 and K_2) provided insight into the contribution to adsorption from the vapor phase and the liquid phase. The theoretical predictions from the surface equation of state agreed well with the experimental data from the three systems.

To model the dynamic adsorption behavior of these systems the equilibrium adsorption isotherm was extended to cover unsteady-state conditions through the creation of a new kinetic transfer equation. As with the adsorption isotherm, the kinetic transfer equation contained expressions for adsorption and desorption on both sides of the interface. The equation was validated against dynamic surface tension data from 1-butanol and 1-hexanol. The model predictions were fit to the experimental data using the vapor phase adsorption rate constant (k_a^g) as a fitting parameter. The model predictions from the transfer equation fit the dynamic surface tension data for the two alcohols well. The only exceptions occurred when the concentration difference between the drop solution and the environment solution was the largest. The deviations may be caused by interactions between adsorbed surfactant molecules due to the elevated interfacial concentration.

Although, based on the model assumptions the adsorption rate constants (k_a^g and k_a^l) should be constant for a given surfactant, a significant variance was detected in the values obtained for different surfactant concentrations. The variation was magnified due to the wide range of concentrations studied. However, specific concentration regions, consistent across both

systems, were identified where the deviations seemed to be most prevalent. Thus, application of the model is best suited for data where these specific regions are avoided.

Chapter 6
Conclusions and Future Work

6.1 Conclusions

This thesis represents a comprehensive investigation on surfactant adsorption and surface tension of slightly volatile, organic amphiphiles in aqueous solution. The research illustrates the influence of simultaneous liquid and vapor phase surfactant adsorption on the interfacial properties of a liquid solution, particularly the surface tension. The following section highlights some of the main conclusions based on the results of the current work.

6.1.1 Conclusions Based on Experimental Work

The Axisymmetric Drop Shape Analysis-Profile (ADSA-P) method was used to measure the dynamic surface tension of a number of organic amphiphiles in aqueous solution. The compounds investigated by this method included 1-butanol, 1-hexanol, 1-octanol, 1-decanol, 1-octanoic acid, and 1-octylamine. In general it was found that the overall trend of the surface tension for these systems seemed to be controlled by the concentration difference between the vapor phase, exerted by the environment solution, and the drop solution. If the concentration of the drop solution was greater than the environment solution the surface tension increased as surfactant was transferred across the interface into the vapor phase. If the concentration of the environment solution was greater than the drop solution the surface tension decreased as surfactant adsorbed at the interface from the vapor phase. If the two concentrations were equal the surface tension remained essentially constant as there was no driving force for molecular transfer. Furthermore, for each environment solution

concentration, a similar final, constant surface tension was attained by each profile regardless of the concentration of the drop solution. This indicates that initially the surface tension was determined by a combination of adsorption from the liquid and the vapor phase, whereas the final steady-state surface tension was determined primarily by adsorption from the vapor. The results are in contrast to data from traditional non-volatile surfactants where the surface tension is mainly controlled by liquid phase adsorption.

The surface tension results from the 1-alcohols were used to explore the effect of the carbon chain length on the observed phenomenon. For 1-butanol, 1-hexanol, and 1-octanol the results were all very similar. However, for 1-decanol some significant differences were observed. During the initial stages of the experiments there were signs that the diffusion process was more prominent for decanol compared to the previous systems. Most notably the initial surface tension values were closer to the surface tension of pure water, and the surface tension decreased initially for the positive concentration difference cases. The results illustrate that increasing the carbon chain length can slow the diffusion process to the point where it is manifested in the surface tension results. However, similar to the other alcohols, the final steady-state surface tension for 1-decanol was found to be independent of the drop solution concentration.

The surface tension results from the two additional organic compounds (1-octanoic acid and 1-octylamine) were used to determine whether the results were limited to alcohol systems or if they were more general in nature. It was found that the octanoic acid results were very similar to the alcohols, with the only notable difference being the extended time-scale for

equilibration. For octylamine some differences were observed for the cases where the environment solution was of intermediate concentration. However, due to the similarities across all of the systems studied it is suspected that the volatile, organic compounds considered in the current study may represent a rather general group of molecules whose surface behavior is unique to that of conventional, non-volatile, or even many volatile surfactants.

The Wilhelmy plate method was used to measure the dynamic surface tension of select cases from the 1-octanol and 1-butanol systems. This served as a verification of the results obtained by the ADSA-P method. Although some differences were observed in the surface tension values, the overall trend was reproduced in each case. This proves the results are not a product of the method used, and increases the confidence in the ADSA-P surface tension results.

To probe the behavior of the pendant drop interface at steady-state conditions, several cases of the 1-octanol system were subjected to a sudden change in drop volume to disrupt the liquid interfacial structure. For the expansion experiments, when the concentration of the drop solution was greater than the environment solution, the surface tension exhibited a rapid decrease, followed by a gradual increase back to the "equilibrium" value prior to the expansion. This is due to the sudden increase in surfactant concentration at the interface during the expansion caused by the disruption of the interfacial energy barrier as fresh solution from the bulk is forced to the surface.

A possible consequence of the observed surface tension phenomenon was illustrated through the measurement of time-dependent contact angle for the 1-octanol solutions. It was found that, for the highest solution concentrations, the contact angle exhibited the expected increase over time corresponding to the increase in surface tension measured by the ADSA-P method. For the lower solution concentrations the contact angle remained essentially constant over the duration of the experiments. For these cases the increase in surface tension was not sufficient to overcome the 'pinning' of the three-phase contact line caused by surface roughness and heterogeneity of the solid surface.

6.1.2 Conclusions Based on Theoretical Analysis

An empirical model was proposed to determine the relationship between the steady-state surface tension and the concentration of the drop and environment solutions. The purpose of the empirical model was to investigate the influence of adsorption from the vapor phase and the liquid phase on the surface tension at both initial and final steady-state conditions. The model was applied to 1-octanol surface tension data from a two-factor, rotatable central composite design (CCD) of experiment. It was found that initially both drop and environment solution concentrations were significant in predicting the surface tension. However, at final steady-state conditions the surface tension was determined to be a quadratic function of the environment solution concentration. The statistical results were consistent with the observations made based on the experimental study that the final steady-state surface tension is independent of the drop solution concentration.

To accurately describe the adsorption behavior of the organic amphiphiles at steady-state conditions a modified equilibrium adsorption isotherm was derived based on the classic

Langmuir analysis. In the derivation of the isotherm both sides of the interface were considered simultaneously and thus, the equation contains expressions for adsorption and desorption in the vapor phase and the liquid phase. The modified isotherm was combined with the Gibbs adsorption equation to create a new surface equation of state capable of predicting the steady-state surface tension as a function of the surfactant concentration in the drop solution and the environment solution. The surface equation of state was used to generate the equilibrium parameters (Γ_∞, K_1, and K_2) for butanol, hexanol, and octanol through nonlinear regression with experimental surface tension data. The parameters were used to explain the adsorption behavior of these surfactants at initial and final steady-state conditions. In all cases the predicted steady-state surface tension values, corresponding to the equilibrium parameter values, agreed well with the experimental data.

To model the adsorption dynamics of the systems studied in this research a new kinetic transfer equation was developed by extending the analysis of the modified adsorption isotherm to unsteady-state conditions. The transfer equation is capable of simulating simultaneous adsorption/desorption from both sides of the interface during dynamic equilibration, and is consistent with the modified adsorption isotherm at steady-state conditions. The transfer equation was validated against dynamic surface tension data from 1-butanol and 1-hexanol. The model was optimized through a nonlinear regression routine using the vapor phase adsorption rate constant (k_a^g) as a fitting parameter. The theoretical predictions agreed well with the experimental data from the two alcohols. The only exceptions occurred when the concentration difference between the drop solution and the

environment solution was the largest. The deviations may be caused by interactions between adsorbed surfactant molecules at the interface.

A significant variance was observed in the values of the adsorption rate constants (k_a^g and k_a^l) corresponding to the theoretical predictions from the kinetic transfer equation. The variance was due to the limitations associated with empirical-type models with adjustable fitting parameters, and was magnified due to the wide range of surfactant concentrations studied. Specific concentration regions, consistent across both systems, were identified where the deviations seemed to be most prevalent. If these conditions are avoided the model succeeds in predicting the experimental data and generating reasonable rate constant values. Therefore, application of the model is best suited for data where these specific regions are avoided.

The results from the theoretical investigation illustrate the importance of vapor phase adsorption when studying the surface properties of this class of common organics during both steady-state and dynamic conditions. The modified Langmuir adsorption isotherm and corresponding kinetic transfer equation can be applied to volatile surfactant systems where liquid and vapor phase adsorption contribute simultaneously to the interfacial surfactant concentration. The adsorption isotherm, surface equation of state, and kinetic transfer equation developed in this research are the first of their kind capable of accounting for dual adsorption and desorption from both sides of the vapor/liquid interface. Consequently, they can be applied to systems where conventional equations do not apply.

Based on the results from the experimental and theoretical sections it is speculated that the behavior of the interface at steady-state conditions may be rather unique to what conventional wisdom would dictate. Although one may expect the final steady-state concentration of the two liquid phases (drop and environment) to be equal, the expansion and consecutive drop experiments proved this to be false. The surface tension at the final steady-state is characteristic of the concentration of the environment solution and not a concentration intermediate to the initial concentrations of the two liquid phases. This leads us to believe that although the vapor phase dominates the behavior of the interface at the final steady-state, the drop solution maintains its initial concentration. A highly structured, hydrogen bonded surfactant network may be forged on the liquid side of the interface hindering the transfer of molecules from the bulk to the surface. A disturbance in the system, illustrated in the expansion and consecutive drop experiments, causes a collapse in the interfacial structure allowing the surfactant to reach the interface. The increase in concentration at the surface results in a decrease in the surface tension. Following the disruption the surface tension begins to recover as the vapor phase resumes control over the interfacial properties and the surfactant network is reestablished.

6.2 Recommendations for Future Work

The following are some recommendations for future work based on the results and conclusions of the current research.

6.2.1 Future Experimental Work

The dynamic surface tension profiles from additional surfactants should be measured to explore the breadth of the observed phenomenon. The surfactants studied in this thesis are all

similar in structure (i.e. linear hydrocarbon chain with a polar group attached at the first carbon position). Thus, it would be of interest to investigate other volatile organic amphiphiles with different structures. Some possible areas of interest include; components with multiple polar groups, polar group displaced towards the interior of the hydrocarbon chain, branched chain amphiphiles as opposed to linear, and amphiphiles with other polar groups.

The time-dependent contact angle results should be improved. Currently the results include one surfactant with limited experimental conditions. The sensitivity of the experiments was very low due to the limitations associated with the substrate chosen as the solid surface. A change in contact angle was observable only when the surface tension changed drastically. Using a substrate with a smooth, uniform surface layer could significantly improve the sensitivity of the measurements. The substrate in question must be moderately hydrophobic to give a finite contact angle for the aqueous solutions. Increasing the sensitivity of the contact angle measurement would improve the current results and also allow for the study of different experimental conditions (i.e. different environment solution concentrations) where the change in surface tension is more subtle. Other surfactants could also be investigated.

Additional surface characterization techniques should be investigated to further the understanding of this unique phenomenon. Although this research represents a significant advance in surface science research, there are still many questions remaining. Exploring different experimental techniques may shed some light on these areas of interest. First, the surface tension experiments should be run using a method capable of measurements at very

short adsorption times. This is the one limitation of the ADSA-P method and recording the surface tension at the millisecond to second range may provide a better understanding of the underlying mechanisms involved in the adsorption process. Also, a technique such as Brewster Angle Microscopy (BAM), Infrared Reflection Adsorption Spectroscopy (IRRAS), or X-Ray or Neutron Scattering could be utilized to help characterize the structure, orientation, and composition of surfactant at the interface. This information would vastly improve the understanding of the behavior of the surfactants at the interface and possibly confirm or disprove the energy barrier hypothesis as an explanation to the loss of molecular exchange from the liquid phase at steady-state conditions.

6.2.2 Future Theoretical Work

The equilibrium adsorption isotherm and kinetic transfer equation should be modified to account for molecular interactions between surfactant molecules at the interface. It has been reported that alcohol molecules exhibit a cooperative effect for adsorption at high surfactant concentrations due to intermolecular attraction. The cohesive forces among the adsorbed molecules raise the energy barrier for desorption into the bulk and thus, lower the rate of desorption. Including an activation energy-type concept which incorporates the effect of increasing surface concentration on the net rate of adsorption at the interface may improve the accuracy of the model predictions. It is possible that some of the discrepancies between the theoretical predictions from the adsorption isotherm or transfer equation may be caused by the failure to account for such interactions.

The dynamic surface tension model should be extended to allow for the simulation of mixed diffusion/transfer-controlled adsorption. Although in this research the kinetic transfer

equation was solved independently to model transfer-controlled adsorption, it may also be coupled with the diffusion equation to describe mixed control systems. This requires the simultaneous solution of the diffusion equation to describe the transport of molecules from the bulk to the subsurface, and the transfer equation to describe the adsorption/desorption step. This modification would greatly increase the robustness and applicability of the model. However, it would also significantly increase the complexity and require the knowledge of additional surfactant properties such as the vapor and liquid phase diffusion coefficients. Possible applications of the advanced model would include alcohols and other similar amphiphiles with longer carbon chains where diffusion effects become more important.

References

1. Dickinson, M., *Animal locomotion: How to walk on water.* Nature, 2003. **424** (6949): p. 621-622.

2. Hu, D.L., B. Chan, and J.W.M. Bush, *The hydrodynamics of water strider locomotion.* Nature, 2003. **424** (6949): p. 663-666.

3. Charlson, R.J., J.H. Seinfeld, A. Nenes, M. Kulmala, A. Laaksonen, and M.C. Facchini, *ATMOSPHERIC SCIENCE: Reshaping the Theory of Cloud Formation.* Science, 2001. **292** (5524): p. 2025-2026.

4. Serrano, A.G. and J. Perez-Gil, *Protein-lipid interactions and surface activity in the pulmonary surfactant system.* Chem. Phys. Lipids, 2006. **141** (1-2): p. 105-118.

5. Sun Young, P., R.E. Hannemann, and E.I. Franses, *Dynamic tension and adsorption behavior of aqueous lung surfactants.* Colloids and Surfaces B (Biointerfaces), 1999. **15** (3-4): p. 325-38.

6. Brodland, G.W., *The Differential Interfacial Tension Hypothesis (DITH): A comprehensive theory for the self-rearrangement of embryonic cells and tissues.* J. Biomech. Eng., 2002. **124** (2): p. 188-197.

7. Brodland, G.W. and H.H. Chen, *The mechanics of cell sorting and envelopment.* J. Biomech., 2000. **33** (7): p. 845-51.

8. Bruinink, C.M., M. Peter, M. De Boer, L. Kuipers, J. Huskens, and D.N. Reinhoudt, *Stamps for submicrometer soft lithography fabricated by capillary force lithography.* Advanced Materials, 2004. **16** (13): p. 1086-1090.

9. Quake, S.R. and A. Scherer, *From Micro- to Nanofabrication with Soft Materials.* Science, 2000. **290** (5496): p. 1536-1540.

10. Vyawahare, S., K.M. Craig, and A. Scherer, *Patterning Lines by Capillary Flows.* Nano Lett., 2006. **6** (2): p. 271-276.

11. Liou, T.M., K.C. Shih, S.W. Chau, and S.C. Chen, *Three-dimensional simulations of the droplet formation during the inkjet printing process.* International Communications in Heat and Mass Transfer, 2002. **29** (8): p. 1109-18.

12. Regan, B.C., S. Aloni, K. Jensen, and A. Zettl, *Surface-tension-driven nanoelectromechanical relaxation oscillator.* Appl. Phys. Lett., 2005. **86** (12): p. 123119-1.

13. Adamson, A.W. and A.P. Gast, *Physical Chemistry of Surfaces*. 6 ed. 1997, New York, NY: John Wiley & Sons, Inc.

14. Neumann, A.W. and J. Spelt, K., *Applied Surface Thermodynamics*. Surfactant science series v. 63. 1996, New York, NY: Marcel Dekker, Inc.

15. Chattoraj, D.K. and K.S. Birdi, *Adsorption and the Gibbs Surface Excess*. 1 ed. 1984, New York, NY: Plenum Press.

16. Hommelen, J.R., *The elimination of errors due to evaporation of the solute in the determination of surface tensions.* J. Colloid Sci., 1959. **14** (4): p. 385-400.

17. MacLeod, C.A. and C.J. Radke, *Surfactant exchange kinetics at the air/water interface from the dynamic tension of growing liquid drops.* J. Colloid Interface Sci., 1994. **166** (1): p. 73-88.

18. Bleys, G. and P. Joos, *Adsorption kinetics of bolaform surfactants at the air/water interface.* J. Phys. Chem., 1985. **89** (6): p. 1027 - 1032.

19. Chang, C.H. and E.I. Franses, *Modified Langmuir-Hinselwood kinetics for dynamic adsorption of surfactants at the air/water interface.* Colloids Surf., 1992. **69** (2-3): p. 189-201.

20. Chang, C.H. and E.I. Franses, *Dynamic tension behavior of aqueous octanol solutions under constant-area and pulsating-area conditions.* Chem. Eng. Sci., 1994. **49** (3): p. 313-325.

21. Fainerman, V.B. and R. Miller, *Adsorption kinetics of short-chain alcohols at the water/air interface: Diffusion-controlled adsorption under the conditions of a nonequilibrium surface layer.* J. Colloid Interface Sci., 1996. **178** (1): p. 168.

22. Kuffner, R.J., *The measurement of dynamic surface tensions of solutions of slowly diffusing molecules by the maximum bubble pressure method.* J. Colloid Sci., 1961. **16** (5): p. 497-500.

23. Lin, S.Y., T.L. Lu, and W.B. Hwang, *Adsorption kinetics of decanol at the air-water interface.* Langmuir, 1995. **11** (2): p. 555-562.

24. Lin, S.Y., K. McKeigue, and C. Maldarelli, *Diffusion-Limited Interpretation of the Induction Period in the Relaxation in Surface Tension Due to the Adsorption of Straight Chain, Small Polar Group Surfactants: Theory and Experiment.* Langmuir, 1991. **7** (6): p. 1055 - 1066.

25. Lin, S.Y., W.J. Wang, and C.T. Hsu, *Adsorption kinetics of 1-octanol at the air-water interface.* Langmuir, 1997. **13** (23): p. 6211-6218.

26. Miller, R. and K. Lunkenheimer, *Adsorption kinetics measurements of some nonionic surfactants.* Colloid Polym. Sci., 1986. **264** (4): p. 357-361.

27. Gibbs, J.W., *The Collected Works of J.W. Gibbs*. Vol. 1. 1931, New York, NY: Longmans, Green.

28. Eastoe, J. and J.S. Dalton, *Dynamic surface tension and adsorption mechanisms of surfactants at the air-water interface.* Adv. Colloid Interface Sci., 2000. **85** (2): p. 103-144.

29. Chang, C.H. and E.I. Franses, *Adsorption dynamics of surfactants at the air/water interface: a critical review of mathematical models, data, and mechanisms.* Colloids Surf. A, 1995. **100**: p. 1.

30. Borwankar, R.P. and D.T. Wasan, *Kinetics of Adsorption of Ionic Surfactants at Gas-Liquid Surfaces.* Chem. Eng. Sci., 1986. **41** (1): p. 199-201.

31. Biswas, M.E., *Adsorption Dynamics at Air-Liquid Interfaces*, in *Chemical Engineering*. 2005, University of Waterloo: Waterloo, ON.

32. Ward, A.F.H. and L. Tordai, *Time-dependence of boundary tensions of solutions. I. The role of diffusion in time-effects.* J. Chem. Phys., 1946. **14**: p. 453-461.

33. Fainerman, V.B., A.V. Makievski, and R. Miller, *The Analysis of Dynamic Surface-Tension of Sodium Alkyl Sulfate-Solutions, Based on Asymptotic Equations of Adsorption Kinetic-Theory.* Colloids Surf. A, 1994. **87** (1): p. 61-75.

34. Langmuir, I., *The Adsorption of Gases on Plane Surfaces of Glass, Mica and Platinum.* J. Am. Chem. Soc., 1918. **40** (9): p. 1361-1403.

35. Damos, F.S., R.C.S. Luz, A.A. Sabino, M.N. Eberlin, R.A. Pilli, and L.T. Kubota, *Adsorption kinetic and properties of self-assembled monolayer based on mono(6-deoxy-6-mercapto)-β-cyclodextrin molecules.* Journal of Electroanalytical Chemistry, 2007. **601** (1-2): p. 181-193.

36. Kraegel, J., R. Wuestneck, F. Husband, P.J. Wilde, A.V. Makievski, D.O. Grigoriev, and J.B. Li, *Properties of mixed protein/surfactant adsorption layers.* Colloids and Surfaces B: Biointerfaces, 1999. **12** (3-6): p. 399-407.

37. Sudah, O.S., G. Chen, and Y.C. Chiew, *Adsorption of single component and binary mixtures of protein and surfactants at the oil-water interface.* Colloids and Surfaces B: Biointerfaces, 1999. **13** (4): p. 195-202.

38. Joos, P. and G. Serrien, *Adsorption-Kinetics of Lower Alkanols at the Air Water Interface - Effect of Structure Makers and Structure Breakers.* J. Colloid Interface Sci., 1989. **127** (1): p. 97-103.

39. Mysels, K.J., *Maximum bubble pressure method of measuring surface tension, revisited.* Colloids Surf., 1990. **43** (2-3): p. 241-262.

40. Defay, R. and G. Petre, *Dynamic Surface Tension*. Surface and Colloid Science, ed. E. Matijevic. Vol. 3. 1971, New York, NY: John Wiley & Sons, Inc.

41. Harkins, W.D. and F.E. Brown, *Determination of surface tension (free surface energy) and the weight of falling drops: Surface tension of water and benzene by the capillary height method.* J. Am. Chem. Soc., 1919. **41**: p. 499-524.

42. Abraham, M.H. and J. Le, *The correlation and prediction of the solubility of compounds in water using an amended solvation energy relationship.* J. Pharm. Sci., 1999. **88** (9): p. 868 - 880.

43. Yaws, C.L., J.R. Hopper, S.R. Mishra, and R.W. Pike, *Solubility and Henry's Law Constants for Amines in Water.* Chem. Eng. (N.Y.), 2001. **108** (8): p. 84-88.

44. Yaws, C.L., J.R. Hopper, S.D. Sheth, M. Han, and R.W. Pike, *Solubility and Henry's law constant for alcohols in water.* Waste Management, 1998. **17** (8): p. 541-547.

45. Ambrose, D. and N.B. Ghiassee, *Vapour pressures and critical temperatures and critical pressures of some alkanoic acids: C1 to C10.* The Journal of Chemical Thermodynamics, 1987. **19** (5): p. 505-517.

46. Munday, E.B., J.C. Mullins, and D.D. Edie, *Vapor Pressure Data for Toluene, 1-pentanol, 1-butanol, Water, and 1-propanol and for the Water and 1-propanol System from 273.15 to 323.15 K.* J. Chem. Eng. Data, 1980. **25** (3): p. 191-194.

47. Nasirzadeh, K., R. Neueder, and W. Kunz, *Vapor pressure determination of the aliphatic C5 to C8 1-alcohols.* J. Chem. Eng. Data, 2006. **51** (1): p. 7-10.

48. Steele, W.V., R.D. Chirico, S.E. Knipmeyer, A. Nguyen, N.K. Smith, and I.R. Tasker, *Thermodynamic Properties and Ideal-Gas Enthalpies of Formation for Cyclohexene, Phthalan (2,5-Dihydrobenzo-3,4-furan), Isoxazole, Octylamine, Dioctylamine, Trioctylamine, Phenyl Isocyanate, and 1,4,5,6-Tetrahydropyrimidine.* J. Chem. Eng. Data, 1996. **41** (6): p. 1269-1284.

49. Rotenberg, Y., L. Boruvka, and A.W. Neumann, *Determination of surface tension and contact angle from the shapes of axisymmetric fluid interfaces.* J. Colloid Interface Sci., 1983. **93** (1): p. 169-183.

50. del Rio, O.I. and A.W. Neumann, *Axisymmetric drop shape analysis: Computational methods for the measurement of interfacial properties from the shape and dimensions of pendant and sessile drops.* J. Colloid Interface Sci., 1997. **196** (2): p. 136.

51. Wu, N., J. Dai, and F.J. Micale, *Dynamic Surface Tension Measurement with a Dynamic Wilhelmy Plate Technique.* J. Colloid Interface Sci., 1999. **215** (2): p. 258-269.

52. Lam, C.N.C., R. Wu, D. Li, M.L. Hair, and A.W. Neumann, *Study of the advancing and receding contact angles: Liquid sorption as a cause of contact angle hysteresis.* Adv. Colloid Interface Sci., 2002. **96** (1-3): p. 169-191.

53. Miller, R., R. Sedev, K.-H. Schano, C. Ng, and A.W. Neumann, *Relaxation of adsorption layers at solution/air interfaces using axisymmetric drop-shape analysis.* Colloids Surf., 1993. **69** (4): p. 209-216.

54. Padday, J.F., *Spreading, wetting, and contact angles.* Journal of Adhesion Science and Technology, 1992. **6** (12): p. 1347-58.

55. Tavana, H., G. Yang, C.M. Yip, D. Appelhans, S. Zschoche, K. Grundke, M.L. Hair, and A.W. Neumann, *Stick-slip of the three-phase line in measurements of dynamic contact angles.* Langmuir, 2006. **22** (2): p. 628-636.

56. Montgomery, D.C., *Design and Analysis of Experiments*. 5 ed. 2001, New York, NY: John Wiley & Sons, Inc.

57. Biswas, M.E., I. Chatzis, M.A. Ioannidis, and P. Chen, *Modeling of adsorption dynamics at air-liquid interfaces using statistical rate theory (SRT).* J. Colloid Interface Sci., 2005. **286** (1): p. 14-27.

58. Castellan, G.W., *Physical Chemistry*. 3 ed. 1983, Menlo Park, CA: Benjamin/Cummings, Inc.

59. Dixit, S., J. Crain, W.C.K. Poon, J.L. Finney, and A.K. Soper, *Molecular segregation observed in a concentrated alcohol-water solution.* Nature, 2002. **416** (6883): p. 829-832.

60. Dixit, S., W.C.K. Poon, and J. Crain, *Hydration of methanol in aqueous solutions: a Raman spectroscopic study.* J. Phys.: Condens. Matter, 2000. **12** (21): p. L323.

61. Joos, P., *Kinetic equations for transfer-controlled adsorption kinetics.* J. Colloid Interface Sci., 1995. **171** (2): p. 399.

62. Hsu, C.-T., M.-J. Shao, and S.-Y. Lin, *Adsorption kinetics of $C_{12}E_4$ at the air-water interface: Adsorption onto a fresh interface.* Langmuir, 2000. **16** (7): p. 3187-3194.